

Protection of Hybrid VSC-MTDC System Against DC Fault

by

Jialin Zhang

A thesis submitted in partial fulfillment of the requirements for the degree of

Master of Science

in

Energy Systems

Department of Electrical and Computer Engineering

University of Alberta

©Jialin Zhang, 2018

# Abstract

Nowadays, the recent trend of high voltage direct current (HVDC) industry is to employ modular multi-level voltage source converter (MMC-VSC) and to build multi-terminal DC (MTDC) systems. The MMC-VSC technology allows VSCs to achieve a higher power rating and the modularity of VSCs provides more flexibility. MTDC systems offer more flexibility and expandability compared with individual point-to-point HVDC connections. It is possible that different types of converters from different manufacturers will be working together in a future MTDC system. In general, MMC-VSCs can be divided into two main categories, full-bridge (FB) VSCs and half-bridge (HB) VSCs depending on the backward current blocking capability. The two kinds of converters have different fault transient responses and require different protection procedures. This thesis focuses on the protection of hybrid MTDC systems that contain VSCs with different fault blocking capabilities against DC faults.

The proposed protection algorithm considered the impact of using the two types of converters in one MTDC system. The DC fault protection algorithm includes a selective fault detection and isolation algorithm and a universal restoration algorithm. The fault detection unit uses DC current derivatives as the criteria to detect potential DC faults. When a pole-to-pole fault occurs, converter-level controllers would block the converters immediately if the preset current derivative thresholds are exceeded. The central-level controller compares the current directions of all the transmission lines and locate the fault. In pole-to-ground fault situations, the central-level controller receives the current measurements from all the converters and determines a pole-to-ground fault by current magnitude analysis. The central-level controller can also analyze the current magnitudes of all the transmission line terminals and locates the pole-to-ground fault.

After the fault isolation, the healthy part of the MTDC system should be restored quickly. A universal restoration algorithm that fits MTDC systems with different types of

converters is proposed, which is simpler and faster compared with the ones proposed in the literature. All the converter stations are controlled individually during the restoration process, avoiding any communication delay. First, fault clearance test is performed by closing an AC breaker which is connected to a HB converter. Second, DC voltage-controlled converters are restored when the voltage of the DC grid reaches the preset values. Finally, the rest of the converters are restored when the DC terminal voltage reaches a stable value. With the proposed restoration algorithm, the four-terminal MTDC test system of this thesis can restore its steady-state operation in one second after isolating the DC fault.

# Acknowledgements

I would like to express my deepest appreciation to my supervisors *Dr. Sahar, P. Azad* and *Prof. Venkata Dinavahi* for their supportive attitude, encouragement, and guidance through my research at the University of Alberta. Undoubtedly, without their constant help and supervision, this dissertation would not have been possible.

It is an honor for me to extend my gratitude to the University of Alberta. With special mentions to *Mr. Ning Lin, Mr. Yashar Kor* and *Dr. Shengjun Huang* for helping me during the two-year research. And my special thanks go to my colleagues and friends at the RTX-Lab and W4-076 with whom I had a wonderful time during my M.Sc. program.

I would like to thank my parents and girlfriend for their great understandings and supports throughout my research.

# Table of Contents

<b>1 Introduction</b>	<b>1</b>
1.1 Background	1
1.2 Challenges	3
1.3 Literature Review	4
1.3.1 Selective Fault Detection	4
1.3.2 Fault Transient Response of VSC-MTDC Systems	5
1.3.3 Post-Fault Restoration	5
1.4 Motivation of This Work	6
1.5 Thesis Contribution	6
1.6 Thesis Outline	6
<b>2 MTDC System Modeling, Control and Protection</b>	<b>8</b>
2.1 Modeling of VSCs	8
2.2 Four-Level Control Hierarchy	11
2.3 Test Systems	14
2.3.1 Point-to-Point HVDC Test System	14
2.3.2 Four-Terminal MTDC Test System	15
2.3.3 Power Flow Control	16
2.3.4 Converter Built-in Protection Unit	17
2.3.5 High Voltage DCCBs	18
2.3.6 Backup Protection	18
2.4 Summary	19
<b>3 Fault Transient Response of Hybrid DC Systems</b>	<b>20</b>
3.1 Introduction	20
3.2 Pole-to-Pole Fault Transients	21
3.2.1 Fault Transient Response of the Point-to-Point Hybrid HVDC System	22
3.2.2 Fault Transient Response of the Point-to-Point HVDC System with FB Converters	25
3.2.3 Fault Transient Response of the Point-to-Point HVDC System with HB Converters	26

3.2.4	Fault Transient Response of the Hybrid Four-Terminal MTDC System	28
3.3	Pole-to-Ground Fault Transients	30
3.3.1	FB and HB Converter Comparison	31
3.3.2	Fault Transient Response of the Hybrid Point-to-Point HVDC System	34
3.3.3	Fault Transient Response of the Hybrid Four-Terminal MTDC System	34
3.4	Other Factors	38
3.4.1	Fault Impedance	38
3.4.2	Converter Blocking Delay	39
3.5	Summary	40
<b>4</b>	<b>Fault Detection, Isolation and System Restoration of Hybrid MTDC Systems</b>	<b>42</b>
4.1	Fault Detection and Isolation	42
4.2	Restoration of HVDC Systems with FB or HB Converters	44
4.2.1	Restoration Algorithm of HVDC Systems with HB Converters	45
4.2.2	Restoration of HVDC Systems with FB Converters	46
4.3	Universal Restoration Algorithm for Hybrid MTDC Systems	46
4.4	Study Results for the Restoration of the Hybrid DC Systems	51
4.4.1	Fault Clearance Test	51
4.4.2	Restoration of the Hybrid Point-to-Point HVDC System	52
4.4.3	Restoration of the Hybrid MTDC System	54
4.4.4	Restoration Failure	57
4.5	Summary	57
<b>5</b>	<b>Conclusion and Future Work</b>	<b>59</b>
5.1	Conclusion	59
5.2	Thesis Contribution	60
5.3	Direction of Future Work	60
	<b>Bibliography</b>	<b>61</b>

# List of Tables

2.1 Point-to-point HVDC test system specifications . . . . .	15
--	----

## List of Figures

2.1 HB MMC submodule modeling. . . . .	9
2.2 FB MMC submodule modeling. . . . .	10
2.3 VSC-MTDC system control hierarchy. . . . .	12
2.4 Upper-level controller of MMC-VSC. . . . .	13
2.5 Point-to-point HVDC test system. . . . .	14
2.6 Four-terminal MTDC test system. . . . .	16
3.1 Timeline and stages of the pole-to-pole fault transient of the hybrid point-to-point HVDC system. . . . .	22
3.2 DC currents of the converters in the hybrid point-to-point HVDC system during the pole-to-pole fault. . . . .	23
3.3 Current flow path during: (a) stage 2 and (b) stage 3. . . . .	24
3.4 Current flow through the fault impedance during the pole-to-pole fault. . . . .	24
3.5 DC voltages of converters in the hybrid point-to-point HVDC system during the pole-to-pole fault. . . . .	25
3.6 Hybrid point-to-point HVDC system AC side current during the pole-to-pole fault for (a) AC source 1 and (b) AC source 2. . . . .	26
3.7 DC current of HB Converter 2 for various fault impedances. . . . .	26
3.8 Timeline and stages of the pole-to-pole fault transient of the FB point-to-point HVDC system. . . . .	27
3.9 Pole-to-pole fault transient of the point-to-point HVDC system with FB converters: (a) DC voltage of Converter 1 and Converter 2 and (b) DC current of Converter 1 and Converter 2. . . . .	27
3.10 Timeline and stages of the pole-to-pole fault transient of the HB point-to-point HVDC system. . . . .	28
3.11 Pole-to-pole fault transient of the point-to-point HVDC system with HB converters: (a) DC voltage of Converter 1 and Converter 2 and (b) DC current of Converter 1 and Converter 2. . . . .	28
3.12 Timeline and stages of the pole-to-pole fault transient of the hybrid four-terminal MTDC system. . . . .	30

3.13 Pole-to-pole fault transient of the hybrid MTDC system: (a) DC current of Converter 1 and Converter 2 and (b) DC current of Converter 3 and Converter 4.	30
3.14 Pole-to-pole fault transient of the hybrid MTDC system: (a) DC voltage of Converter 1 and Converter 2 and (b) DC voltage of Converter 3 and Converter 4.	31
3.15 Timeline of the pole-to-ground fault transient of FB and HB point-to-point HVDC system.	32
3.16 Pole-to-ground fault transient of the FB and HB point-to-point HVDC system. (a) DC voltage and (b) DC current.	32
3.17 Current flow through fault impedance during the pole-to-ground fault.	32
3.18 DC terminal voltage of Converter 2 caused by the uncontrollable AC source contribution.	33
3.19 Timeline of the pole-to-ground fault transient of the hybrid point-to-point HVDC system.	34
3.20 Pole-to-ground fault transient response of the hybrid point-to-point HVDC system: (a) DC voltage and (b) DC current.	35
3.21 Fault impedance current during the pole-to-ground fault.	35
3.22 Timeline of the pole-to-ground fault transient of the hybrid MTDC system.	35
3.23 Pole-to-ground fault transient current: (a) Converter 1 and Converter 2 and (b) Converter 3 and Converter 4.	36
3.24 Pole-to-ground fault transient of the four-terminal MTDC system: (a) Voltage of Converter 1 and Converter 2 and (b) Real power of Converter 3 and Converter 4.	37
3.25 Timeline of the pole-to-ground fault transient of the hybrid MTDC system.	37
3.26 Pole-to-ground fault current of the four-terminal MTDC system.	37
3.27 Timeline and of the pole-to-ground fault transient of the hybrid MTDC system.	38
3.28 Pole-to-ground fault current of the four-terminal MTDC system.	38
3.29 Total voltage of SMs in one arm: (a) Converter blocking delay of 2 ms and (b) Converter blocking delay of 3 ms.	39
4.1 Fault detection and isolation algorithm.	43
4.2 Restoration timeline of the HB point-to-point HVDC system.	46
4.3 Restoration of HB point-to-point HVDC system: (a) DC voltage of Converter 1 and Converter 2 and (b) Real power of Converter 1 and Converter 2.	47
4.4 Restoration timeline of the FB point-to-point HVDC system.	47
4.5 Restoration of FB point-to-point HVDC system: (a) DC voltage of Converter 1 and Converter 2 and (b) Real power of Converter 1 and Converter 2.	48
4.6 The proposed restoration algorithm.	50

4.7 DC voltage of the four converters during a successful fault clearance test. . . . .	51
4.8 DC voltage of the four converters during a failed fault clearance test. . . . .	52
4.9 The restoration timeline of the hybrid point-to-point HVDC system. . . . .	53
4.10 Restoration of the hybrid point-to-point HVDC system: (a) DC voltage and (b) Real power. . . . .	53
4.11 Trigger diagram in the simulation. . . . .	54
4.12 The restoration timeline of the hybrid four-terminal MTDC system. . . . .	54
4.13 DC voltage of the four converters during restoration. . . . .	55
4.14 Real power of the four converters during restoration. . . . .	56
4.15 The restoration failure timeline of the hybrid four-terminal MTDC system. . . . .	57
4.16 Restoration failure of the hybrid MTDC system: (a) DC voltage of the four converters and (b) DC current of four converters. . . . .	58

## List of Acronyms

<b>AC</b>	Alternating Current
<b>DC</b>	Direct Current
<b>RES</b>	Renewable Energy Source
<b>HVDC</b>	High Voltage Direct Current
<b>LCC</b>	Line-Commutated Converter
<b>VSC</b>	Voltage Source Converter
<b>FB</b>	Full-Bridge
<b>HB</b>	Half-Bridge
<b>MMC</b>	Modular Multi-level Converter
<b>MTDC</b>	Multi-Terminal Direct Current
<b>FACT</b>	Flexible Alternating Current Transmission
<b>STATCOM</b>	Static Compensator
<b>DCCB</b>	Direct Current Circuit Breaker
<b>ACCB</b>	Alternating Current Circuit Breaker
<b>MD</b>	Mechanical Disconnect
<b>PLL</b>	Phase-Lock Loop
<b>PWM</b>	Pulse Width Modulation
<b>PSCAD</b>	Power System Computer-Aided Design
<b>RMS</b>	Root Mean Square
<b>EMT</b>	Electro-Magnetic Transient

# 1

## Introduction

### 1.1 Background

In the past, the power grid relied heavily on fossil fuel-based electricity generations [1]. Nowadays, the increasing energy cost and the deteriorating global environment places a high demand for renewable energy sources (RESs). RESs such as solar and wind farms are widely used in order to reduce the carbon emission and to make economic benefits. RESs are usually widely distributed and are located far away from major cities. One example is the offshore wind farms in the North Sea.

The European Union (EU) has been leading the RES development in the past decade and this trend is expected to continue [2]. EU expects to cut at least 40% of greenhouse gas emissions by 2030, and 80-95% by 2050 compared to that of 1990 [3,4]. To deal with the increasing RESs, transmission grid studies such as e-Highway 2050 [4] and ten-year network development plan are conducted by European Network of Transmission System Operators for Electricity (ENTSO-E) [5]. Both plans point out that high voltage direct current (HVDC) transmission is the preferred technique to connect RESs into the existing power grid.

Point-to-point HVDC transmission has been widely used to economically transmit bulk power generated by RESs over long distances since 1954. HVDC offers many advantages over high voltage alternating current (HVAC) including:

- **Lower losses:** In HVAC transmission, the skin effect would cause an unequally distributed current in the transmission lines. The result is a higher transmission line resistance for AC currents compared with DC currents.

- **Reactive power consumption:** In HVAC transmission, due to the inductive nature of the transmission line, reactive power has to be transmitted along with active power. DC transmission lines only carry active power.
- **Asynchronous AC connection:** HVDC links can be used to connect AC grids with different frequencies. In Europe, this feature allows the interconnection between more countries. In North America, HVDC transmission allows the asynchronous interconnection between the United States and Canada.
- **Long-distance transmission:** There are several factors that limit the distance of HVAC transmission such as reactive power compensation and sub-synchronous resonances [6]. For HVDC systems, the transmission distance is not limited by these factors.
- **Blocking cascading blackouts:** HVDC transmission can prevent cascading blackouts when AC faults occur. One example is that Quebec was able to survive the Northeast blackout of 2003 because of the use of HVDC instead of AC transmission. [7].
- **Construction cost:** AC transmission lines use three conductors, whereas DC transmission lines only use two. The pylon (tower) for HVDC transmission is simpler than those for HVAC transmission. Furthermore, HVDC systems are going to use more cables instead of transmission lines in the future. Although the insulation cost of cables is higher than transmission lines, the use of cables requires less land and labor.
- **Communication interference:** Overhead HVAC transmission lines have conductive or inductive effects, which would cause communication interference along their paths. However, HVDC transmission lines do not cause this problem [8].

Classic or traditional HVDC systems use line commutated converters (LCCs), which employ solid-state switches such as thyristors to replace the preceding mercury-arc valves. The last mercury-arc valve-based HVDC system was shut down in 2012 [9]. The first HVDC transmission line using thyristors is the Eel River 320 MW interconnection between the New Brunswick and Quebec [10]. Currently, a thyristor-based HVDC transmission system of  $\pm 1100$  kV and over 10 GW is under construction in China [11]. Overall, LCC-based HVDC transmission is a mature technology.

With the advancements in power electronics technology, voltage source converter-based HVDC (VSC-HVDC) systems are gaining more recognition and market share because of their reactive power flexibility, better power controllability and higher converter efficiency [12]. The Gotland HVDC Light is the first commercial HVDC transmission based on VSC technology [13]. In North America, many HVDC and FACTS devices are reaching their life expectancies, and may be replaced by VSCs [14].

Nowadays, the recent trend of HVDC industry is to employ modular multi-level voltage source converter (MMC-VSC) and to build multi-terminal DC (MTDC) systems. The state-of-the-art MMC-VSC technology allows VSCs to achieve a higher power rating and the modularity of VSCs provides more flexibility [15]. MTDC systems offer more flexibility and expandability to integrate more RESs [16]. MTDC systems are also more reliable and efficient to share the power between the terminals compared with individual point-to-point HVDC connections [17]. In China, there are several MTDC systems in operation such as the three-terminal 160 kV Nan' Ao grid and the five-terminal 200 kV ZhouShan grid [18]. In Europe, the North Sea neighboring countries have been envisioning an MTDC system since 2010 and several designs have been proposed in [19,20]. However, an MTDC system has not been realized in the North Sea yet. The proposed designs for the North Sea MTDC system requires the integration of the existing converter stations (VSCs) into one grid. China is also planning to expand the existing MTDC systems.

With more RESs integrated, there will be more MMC-VSCs in the DC grid. So, it is possible that different kinds of converters from different manufacturers will be working together in a future MTDC system. There are many variants of MMC submodule (SM) configurations proposed in the literature [21,22]. In general, MMC-VSCs can be divided into two main categories, full-bridge (FB)-VSCs and half-bridge (HB)-VSCs depending on the backward current blocking capability. The MMC SM that can block bi-directional currents is known as FB. Otherwise, the SM is known as HB. When integrating the two kinds of converters into one MTDC system, several technical challenges must be addressed such as power flow control, modeling, and the DC fault protection. This thesis focuses on the DC fault protection of MTDC systems with converters with different fault blocking capability, i.e., FB and HB converters.

## 1.2 Challenges

In MTDC systems, the main challenges related to DC fault protection are:

- To detect the DC fault fast and to protect the electronic components.
- To avoid communication delay in the protection process.
- To select and isolate the faulted transmission line fast.
- To develop high voltage direct current circuit breakers (DCCBs) since mature and economically viable DCCBs are not available yet.
- To restore the healthy part of an MTDC system quickly.

VSCs have many control advantages over LCCs. But VSCs do not have DC fault current blocking capability like LCCs. When a DC fault occurs, the DC side current of a VSC can rise to more than 10 times the rated value, damaging the electronic switches. The vulnerability of VSCs to DC faults requires the protection unit to react quickly and accurately to DC faults. The protection unit should act in four fundamental steps [23]:

- **Fault detection:** Detect a fault based on current magnitude, current rise rate or other criteria.
- **Converter protection:** Take protective actions to protect the power electronic components in the system by interrupting the fault current.
- **Fault isolation:** Isolate the faulted part of the system.
- **Post-fault restoration:** Restore the healthy part of the MTDC system as soon as possible to minimize the impact of the faults and resulting outages.

## 1.3 Literature Review

### 1.3.1 Selective Fault Detection

The fault detection algorithm for VSC-HVDC systems is discussed in the literature for decades [24, 25]. Non-communication-based fault detection or local fault detection algorithms response faster than those using a communication system [24]. A simple method to detect a DC fault is to monitor the DC current of a converter. When the DC current is dangerously high for the converter, the converter should be blocked to protect the switches. Fault detection methods based on monitoring current or voltage magnitudes only work when the current or voltage deviates from the normal value to a certain level. To make the fault detection even faster, current and voltage derivatives can be monitored to detect a DC fault. [26] proposed a fault detection method using AC side measurement. [27] proposed an artificial neural network (ANN) based fault detection algorithm. The Handshaking method proposed in [28] selects the faulted line by the direction of DC current. These fault detection algorithms can be used to detect a DC fault without communication.

The fault detection algorithm in [29] uses traveling wave natural frequency to locate a DC fault. In [30], DC voltage and current are analyzed with Wavelet transform to locate a DC fault. [31] proposed an algorithm based on current and voltage frequency band to locate the fault in a certain protection zone. [25] proposed a selective transient voltage based fault detection and protection algorithm. The proposed method uses transient voltage blocking effect of the supplemental inductor to locate a fault. The above-mentioned methods have been verified in MTDC systems with only one type of converter. Although the algorithms in [25, 29-31] are proven to be selective, they do not take the impact of converter type into consideration.

### 1.3.2 Fault Transient Response of VSC-MTDC Systems

There are many factors that affect the fault transient responses of an MTDC system such as converter type, system configuration, fault type and protective operations. For VSC-MTDC systems, there are several options in terms of configuration and grounding. There are three kinds of MTDC system configurations: asymmetric monopolar, symmetric monopolar and bipolar and two kinds of basic grounding options: low impedance grounding and high impedance grounding [32]. Among these options, symmetric monopolar with high impedance grounding is the most common system configuration [32]. The fault transient of FB MMC-VSCs in a four-terminal MTDC system is studied in [33]. The fault transient of an HVDC system with HB MMC-VSCs is studied in [18, 24]. In [18, 34], the influences of high voltage direct current circuit breakers (DCCBs) on the fault transient responses of point-to-point HVDC links are studied in different system configurations. The studies show that DCCBs can reduce the stress on the converters during DC faults.

### 1.3.3 Post-Fault Restoration

After clearing the DC fault or isolating the faulted part, the healthy part of the MTDC system should be restored as soon as possible. Restoration methods for VSC-HVDC systems using black-start capability are proposed in [35, 36]. However, for MMC-VSCs, the restoration and the black-start methods should be different. The black-start of an MMC involves the charging of capacitors in SMs. However, blocking the converters quickly in fault conditions allows the SMs to keep the charge in the capacitors. So, the black-start methods for VSC-HVDC systems do not fit MMC-based HVDC systems if the converters are blocked quickly. [23] presented a restoration framework for MTDC systems. With the proposed algorithm, a four-terminal MTDC can be restored within 3.6 s without the use of expensive high voltage DCCBs. This framework provided several important principles for the restoration of MTDC systems.

- If high voltage DCCBs are not available in an MTDC system, clearing a permanent DC fault requires the de-energization of the entire DC grid.
- The restoration of an MTDC system should start from a converter which is in charge of controlling the DC voltage.
- Real power-controlled converters can only be restored when the DC voltage is stable.

The restoration algorithm in [23] only considers the MTDC grids with FB (H-bridge) MMCs. A faster restoration algorithm for MTDC systems with only FB MMCs was proposed in [37]. By controlling the individual switches in the SMs and creating short circuit loops through the FB converters, the energy in the MTDC system can be released faster. This method works only when all the converters in the system are FB converters. [28]

proposed a Handshaking method for the restoration of VSC-MTDC systems. The small current injection test of Handshaking method is an effective way to make sure the MTDC system is free of DC faults. Overall, no existing restoration algorithm considers the impact of converters with various fault blocking capabilities in an MTDC system.

## 1.4 Motivation of This Work

Conventional methods to protect MTDC systems do not consider the interoperability challenge, where different types of converters may work together in one MTDC system. The combination of converters with various fault blocking capability makes the fault transient more complex and consequently highly impacts the existing selective fault detection and restoration algorithms. The selective fault detection algorithm proposed in this thesis will not be influenced by the different fault transients caused by the various converters. The existing post-fault restoration algorithms do not consider the complexity of the hybrid MTDC systems, which will have converters with different fault blocking capabilities. To address this challenge, a universal restoration algorithm is required. The universal restoration algorithm should fit all MTDC systems and their future expansion. Furthermore, the universal restoration algorithm should quickly restore an MTDC system.

## 1.5 Thesis Contribution

This thesis focuses on the protection of hybrid HVDC grids with two types of modular multi-level converters (MMCs) including half-bridge (HB) and full-bridge (FB). The two types of converters have different fault transient responses and require different protection procedures to interrupt the fault current. This thesis studies the fault transient response of hybrid MMC-HVDC grids in Chapter 3 and proposes a relaying algorithm based on DC current derivatives to detect various types of faults in such hybrid systems in Chapter 4. Furthermore, Chapter 4 provides a universal restoration algorithm, which restores the hybrid MMC-HVDC grid with any combination of converters with and without fault blocking capability in a short period after isolating the DC faults.

## 1.6 Thesis Outline

The rest of this thesis is organized as follows:

- **Chapter 2: MTDC system modeling, control and protection:** This chapter provides the framework for this research by discussing the modeling and control of MMC-VSCs and MTDC systems. Two test systems are introduced, one is a point-to-point HVDC system and another is a four-terminal MTDC system. The converter control unit in the test system is compatible with three kinds of basic converters: FB

MMCs, HB MMCs and two level VSCs. The MTDC system protection schemes are also briefly discussed.

- **Chapter 3: Fault transient response of hybrid DC systems:** This chapter includes the fault transient studies of MMC-VSCs in the two test systems. The differences between FB and HB MMC-VSCs are compared. The fault transient responses of two kinds of faults, pole-to-ground and pole-to-pole faults are studied individually. Several factors that may influence the fault transient responses are discussed and evaluated via simulations.
- **Chapter 4: Fault detection, isolation and system restoration of hybrid MTDC systems:** This chapter discusses the fault detection and isolation as well as system restoration of hybrid MTDC systems. The fault detection and isolation algorithm is discussed for pole-to-pole and pole-to-ground faults. The restoration algorithms for HVDC systems with FB and HB MMC-VSCs are compared. Combining the restoration algorithms for FB and HB converters, a universal restoration algorithm is proposed. The proposed algorithm is verified in the point-to-point HVDC and MTDC test systems.
- **Chapter 5: Conclusion and future work:** This chapter summarizes the results and contributions of this thesis. Finally, several future research directions are identified.

# 2

## MTDC System Modeling, Control and Protection

This chapter provides an overview of MTDC systems in terms of modeling, power flow control, and important techniques related to MTDC system protection. Section 2.1 discusses the modeling of VSCs. Section 2.2 discusses the four-level controllers for MTDC systems. Section 2.3 introduces two test systems as well as the system control details. Several techniques related to MTDC system protection are also discussed in Section 2.3. Section 2.4 provides a summary of this chapter.

### 2.1 Modeling of VSCs

A hybrid MTDC system consists of VSCs in a variety of configurations, AC sources, and cables or overhead transmission lines. There are seven types of computational models for MMC-VSCs [38].

- **Type 1-Full physics-based models:** All the switches and diodes are represented by their associated differential equations.
- **Type 2-Full detailed models:** Type 2 models use nonlinear resistors to represent diodes and use ideal switches to represent IGBTs.
- **Type 3-Models based on simplified switchable resistances:** Type 3 models use two-value resistors that are selected by gating signals to represent diodes and switches.
- **Type 4-Detailed equivalent circuit models:** Type 4 models are based on Type 3 models with reduced electric nodes that describe the converters.

- **Type 5-Average value models based on switching functions:** In Type 5 models, AC and DC side characteristics are modeled as controlled current and voltage sources with harmonic contents.
- **Type 6-Simplified average value models:** In Type 6 models, the AC and DC sides of VSCs are modeled as controlled current and voltage sources at the fundamental frequency.
- **Type 7-Root Mean Square (RMS) load-flow models:** Type 7 models only provide the steady-state responses of the converters.

The protection algorithms of MTDC systems must be tested and verified via electro-magnetic transient (EMT)-type simulations. Therefore, all the simulations of this thesis have been done in Power Systems Computer Aided Design/Electro Magnetic Transient Design and Control (PSCAD/EMTDC<sup>®</sup>) environment [39]. In this thesis, Type 4 models have been used for EMT simulation of MMC-VSCs in the PSCAD/EMTDC<sup>®</sup> software. In Type 4 models, switches and diodes are represented by two-value resistors. The value of the resistance is controlled by gating signals and the current direction. The capacitors in MMC SMs are modeled as a voltage source and a resistor. The model of a HB MMC SM is shown in Fig. 2.1. Following the Trapezoidal Integration method, a capacitor can be represented as a voltage source and a resistor [38].

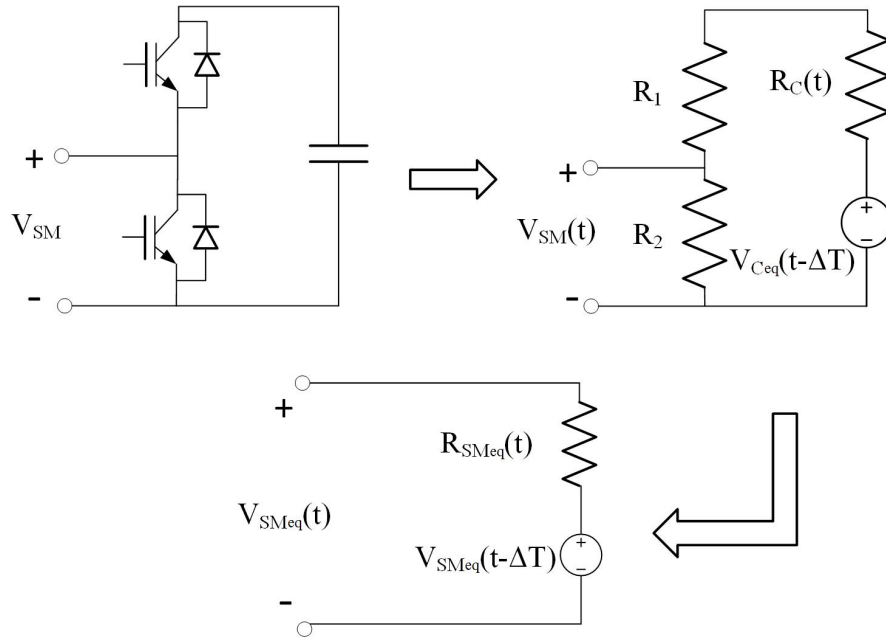


Figure 2.1: HB MMC submodule modeling.

$$V_c(t) = R_c i_c(t) + V_{C_{eq}}(t - \Delta T), \quad (2.1)$$

where

$$R_c(t) = \frac{\Delta T}{2C} \quad \text{and} \quad V_{C_{eq}}(t - \Delta T) = \frac{\Delta T}{2C} i_c(t - \Delta T) + V_c(t - \Delta T) \quad (2.2)$$

The HB SM can be represented by a Thevenin equivalent circuit as shown in Fig. 2.1. The equivalent voltage and resistance are:

$$R_{SM_{eq}}(t) = (R_1(t) + R_c(t)) || R_2(t), \quad (2.3)$$

$$V_{SM_{eq}}(t) = (R_{SM_{eq}}(t)i(t) + V_{SM_{eq}}(t - \Delta T)), \quad (2.4)$$

where

$$V_{SM_{eq}}(t - \Delta T) = V_{C_{eq}}(t - \Delta T) \left( \frac{R_2(t)}{R_2(t) + R_1(t) + R_c(t)} \right) \quad (2.5)$$

Similarly, a FB MMC SM can be represented by the Thevenin Equivalent Circuit as shown in Fig. 2.2. The differences between HB and FB SM equivalent models are the equivalent resistance and voltage source.

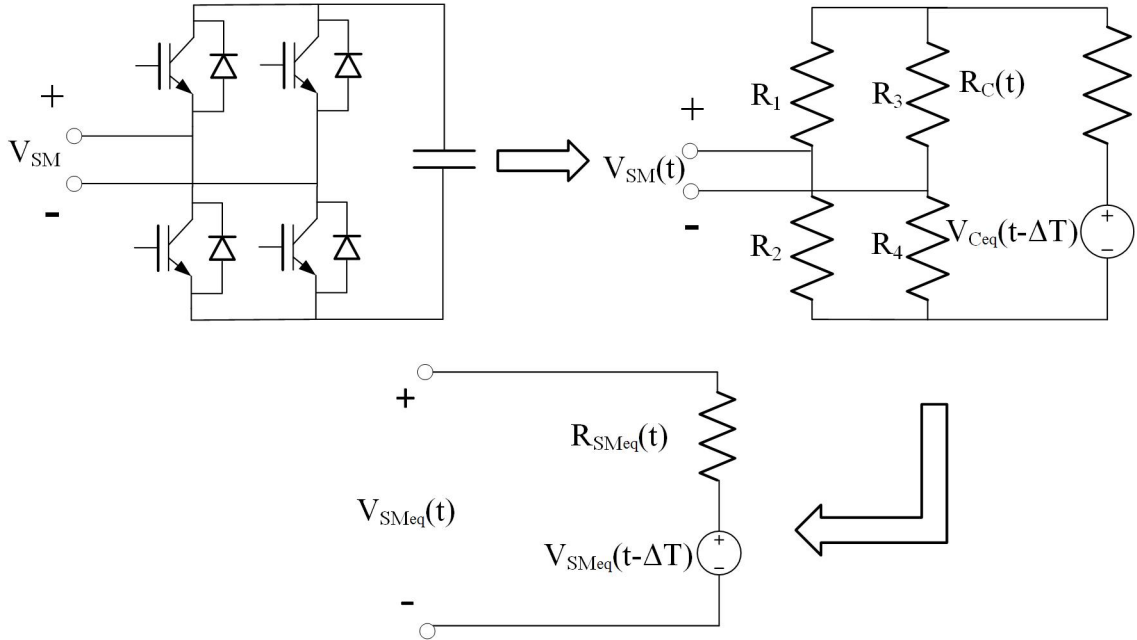


Figure 2.2: FB MMC submodule modeling.

In an MMC-VSC, all SMs in one phase are connected in series and can be replaced by a Thevenin Equivalent Circuit. All the SM resistances and voltage sources are connected in series. The voltage of all the SMs in one arm can be represented by:

$$V_{eq}(t) = \sum_1^n R_{SM_{eq}}(t)i(t) + \sum_1^n V_{SM_{eq}}(t - \Delta T) \quad (2.6)$$

The main advantage of Type 4 model is that it limits the number of nodes in an MMC-VSC. In this case, one arm (upper arm or lower arm) of one converter phase can be represented by only two electric nodes. Type 4 models make the computation much faster than Type 3 models while maintaining a similar simulation accuracy for fault analysis. The details about Type 4 equivalent models are studied in [40].

## 2.2 Four-Level Control Hierarchy

The control unit in an MTDC system consists of four levels:

- System/Central-level control;
- Converter-level control;
- Upper-level control;
- Lower-level control.

The functions of all four levels of the control unit are summarized in Fig. 2.3. The system-level controller or the central-level controller manages all converters and transmission lines in the MTDC system. The central-level controller can decide the blocking or deblocking states of all converters by sending commands to converter-level controllers. The central-level controller can also send commands to converter-level controllers to operate the DC disconnectors and the AC circuit breakers (ACCBs) to isolate a transmission line or a converter. The converter set-points, initialization and protection algorithms are also decided by the central-level controller. When a DC fault occurs in an MTDC system, the central-level controller should receive necessary data from all the converter stations and determine the fault location and type.

Converter-level controllers handle the operation of all the devices in the converter station including the DC disconnectors and the ACCBs. Converter-level controllers follow the commands from the central-level controller. In case of a DC fault, converter-level controllers block the converters and open the ACCBs during severe pole-to-pole faults. Converter-level controllers should report all the operations to the central-level controller.

Converter-level controllers set the converter operation modes as required by the central-level controller. In general, there are two kinds of control modes for a VSC:

- Non-islanded mode, and

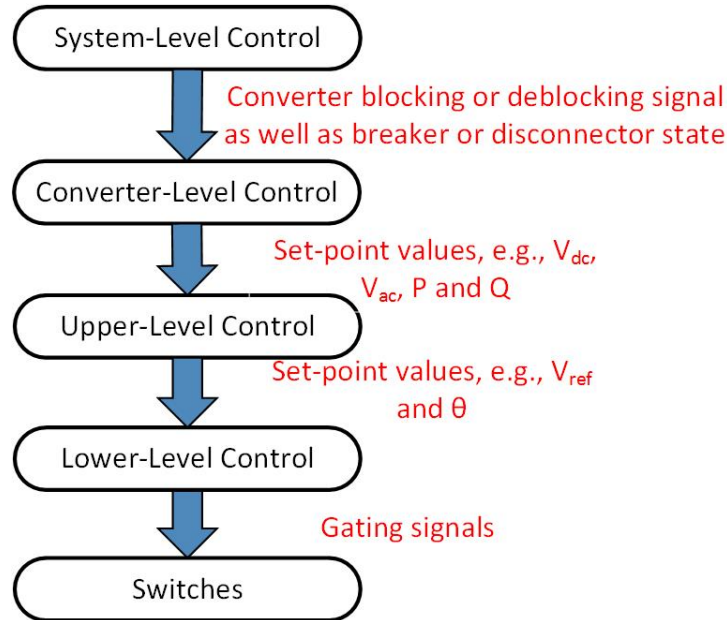


Figure 2.3: VSC-MTDC system control hierarchy.

- Islanded mode.

Islanded mode operation is out of the scope of this thesis. Non-islanded mode controls are based on current vector control, which regulates the direct (d) and quadrature (q) components of the AC voltage and current. The d and q components of AC current correspond to active and reactive power controls, respectively. Active power control loop can operate in:

- DC voltage control mode, or
- Real power control mode.

Reactive power control loop can operate in:

- AC voltage control mode, or
- Reactive power control mode.

The control loop for upper-level controllers is shown in Fig. 2.4. Converter-level controllers will provide the mode setting and all the set-points required by upper-level controllers. A phase-lock loop (PLL) generates a reference frame angle  $\theta$  by locking onto the AC voltage  $V_{abc}$  at the point of common-coupling (PCC) with the grid. Three phase AC currents and voltages are transformed into the dp frame using the reference frame angle  $\theta$  to produce the d and q reference currents and voltages,  $i_d$ ,  $i_q$ ,  $v_d$  and  $v_q$ . The reference values of  $i_{dref}$  and  $i_{qref}$  are produced by active and reactive power control loops, respectively. The outputs from the upper-level controllers are the reference values for AC side

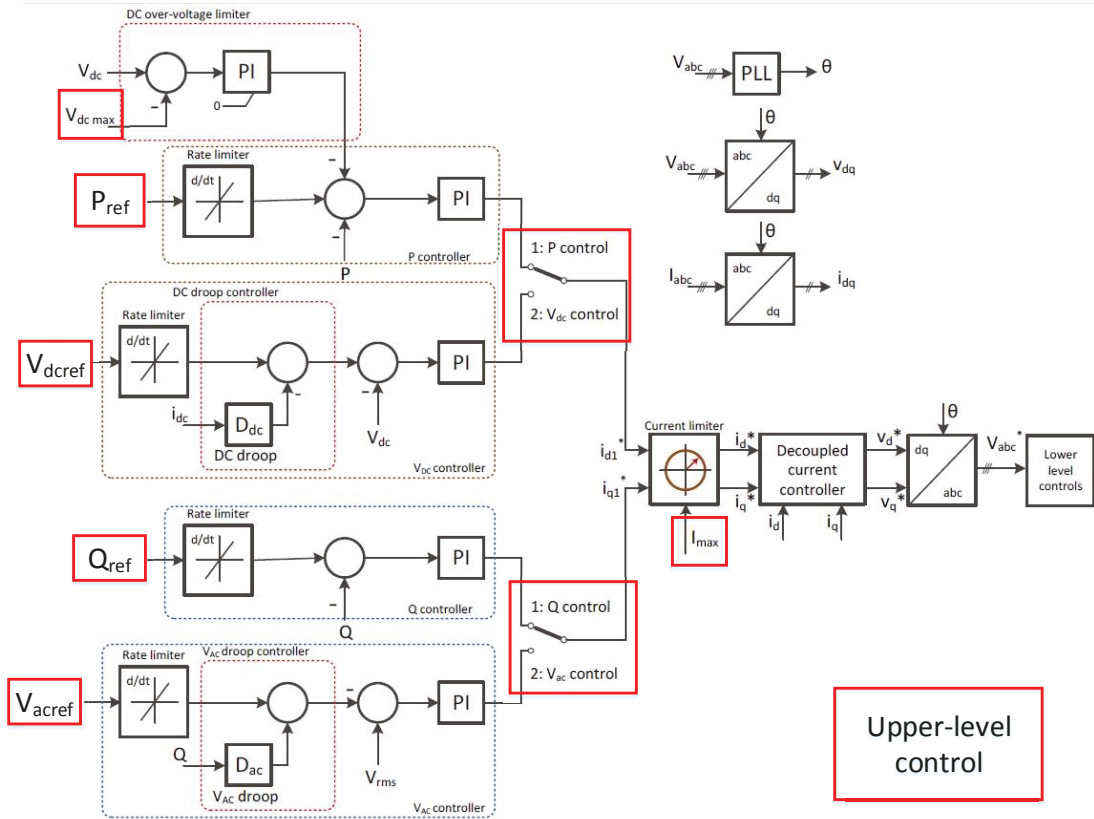


Figure 2.4: Upper-level controller of MMC-VSC.

voltage and phase angle. This information is sent to the lower-level controllers.

Lower-level controllers will send the firing signals to converter switches to generate the AC waveforms that are requested by the upper-level controllers. Lower-level controllers for MMC-VSCs can employ the capacitor voltage balancing [41], nearest level control [42] or pulse width modulation (PWM) [43] techniques to select the SMs that should be turned on in each arm. At the same time, the capacitor voltages of all the SMs should be maintained close to the average voltage value.

The central-level controller and converter-level controllers can both control the blocking and deblocking of a converter and the state of ACCBs and DC disconnectors. The main differences between these two controllers are:

- Converter-level controllers are responsible to protect all the switches in the converter stations. In fault situations, converter-level controllers can take independent operations to protect the devices fast.
- The central-level controller receives information from all the converters while converter-

level controllers only have access to local information.

- In case of conflicting commands from the central-level and converter-level controllers, the central-level controller has the priority.
- Converter-level controllers do not communicate with each other.

## 2.3 Test Systems

There are two test systems used in this thesis, a point-to-point HVDC system and a four-terminal MTDC system. The test systems have a mono-polar, symmetric configuration. The positive and negative DC terminals of all the converters are grounded via 1,000 k $\Omega$  resistors. The active power control loop can be set to DC voltage or real power control mode and the reactive power control loop can be set to AC voltage or reactive power control mode.

### 2.3.1 Point-to-Point HVDC Test System

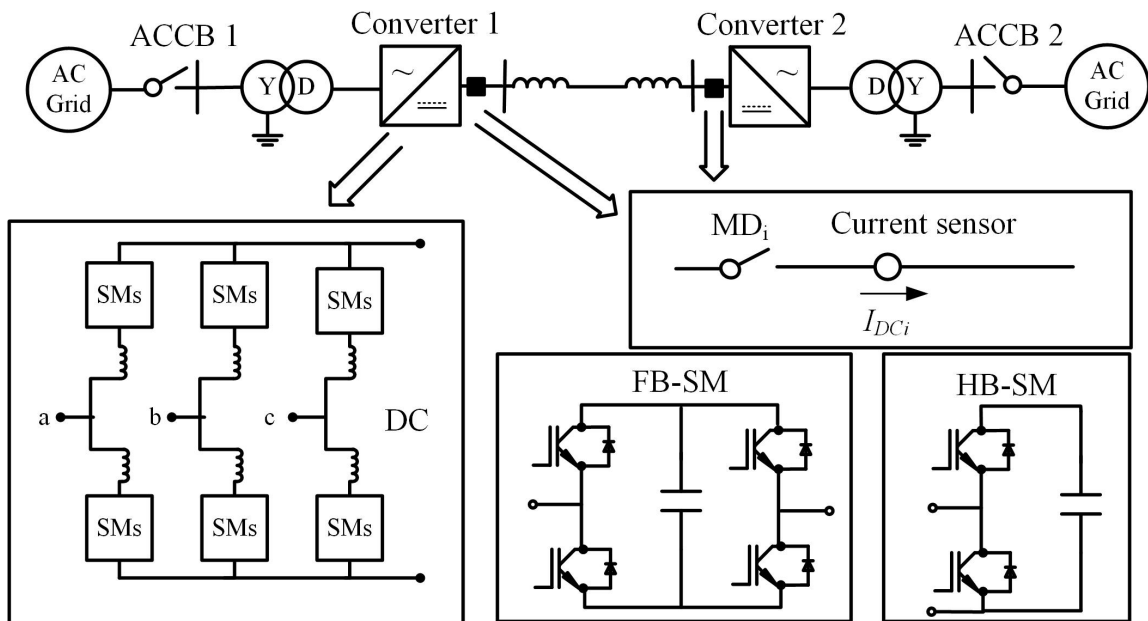


Figure 2.5: Point-to-point HVDC test system.

The point-to-point HVDC test system is shown in Fig. 2.5. The two converters in the test system are named Converter 1 and Converter 2 and they can be based on FB or HB SMs. Therefore, the test system can be used in three configurations based on the converter type: two HB converters, one FB converter and one HB converter or two HB converters. In a point-to-point HVDC system, there should be one converter in DC voltage control mode

and another converter in real power control mode. In a hybrid point-to-point HVDC system with one FB and one HB converter, the FB converter should be in charge of controlling the DC voltage. This allows for a more controllable the startup and restoration. The startup and restoration processes require the DC voltage-controlled converter to energize the DC system. Since the FB converter remains connected to the system during the fault clearance, the restoration process will be expedited. The system specifications are shown in Table 2.1.

Table 2.1: Point-to-point HVDC test system specifications

Specifications	Converter 1	Converter 2
DC side voltage	640 kV	640 kV
DC side power	900 MW (Rectifier)	-900 MW (Converter)
DC side current	1.6 kA (Rectifier)	-1.6 kA (Converter)
Converter rated power	1000 MW	1000 MW
AC source voltage	230 kV	230 kV
Transformer ratio	230:370	230:370

### 2.3.2 Four-Terminal MTDC Test System

The second test system used in this thesis is a four-terminal MTDC system. This system is used as a hybrid four-terminal MTDC system with two configurations. The hybrid MTDC system 1 has two FB converters and two HB converters. The hybrid MTDC system 2 has one FB converter and three HB converters. The length of all the transmission lines is 400 km. In general, an MTDC system should have at least one converter in DC voltage control mode and one converter in real power control mode. Parameters of the converters are the same as the point-to-point test system. During the normal operation, AC grids 1 and 4 inject power to the DC grid and AC grids 2 and 3 absorb power from the DC grid. Therefore, the DC current and power of Converter 1 and Converter 4 are the same as these of Converter 1 in the point-to-point system. The DC current and power of Converter 2 and 3 are the same as these of Converter 2 in the point-to-point system. Each converter station includes a transformer, a filter, an AC-DC converter and several current sensors in series with DC disconnectors on all the transmission line terminals as shown in Fig. 2.6.

The electrical parameters of a cable or an overhead transmission line are frequency-dependent. The model of cables and overhead transmission lines for protection studies should be based on the traveling wave theory. In [44], a fundamental formulation of frequency dependent models of transmission lines is provided. In the test systems of this thesis, transmission lines are represented bases on the PSCAD/EMTDC<sup>®</sup> embedded

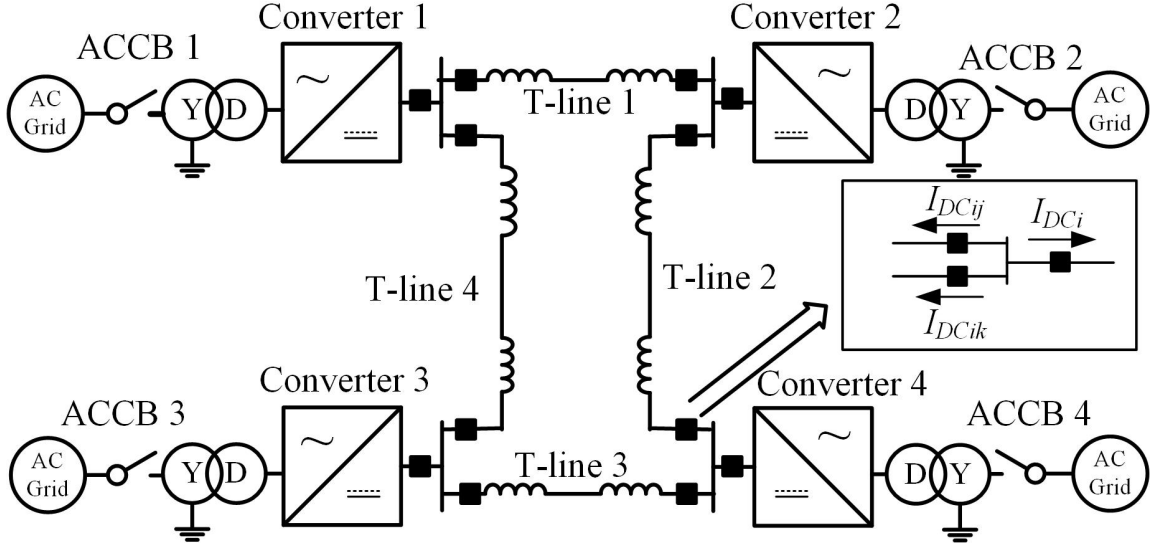


Figure 2.6: Four-terminal MTDC test system.

frequency-dependent model, which is studied in [45,46]. The AC grids in the test systems are three-phase 230 kV, 60 Hz voltage sources.

### 2.3.3 Power Flow Control

In the point-to-point HVDC test system, one converter should be in DC voltage control mode and another converter should be in real power control mode. The power flow control between the two converters is achieved by changing the set-point of the real power-controlled converter.

In the four-terminal MTDC test system, there should be at least one converter in DC voltage control mode. In the case studies of this thesis, Converter 1 and Converter 4 are in DC voltage control mode and Converter 2 and Converter 3 are in real power control mode. The power absorptions of Converter 2 and Converter 3 are controlled by the set-points. The power injections among the rest of the converters are controlled by adjusting the DC voltages at the DC terminals. In the test system, the DC voltage of Converter 1 is set to 640 kV. By changing the DC voltage setting of Converter 4, the power flow of all the converters can be controlled.

In the four-terminal test system, the voltage and power set-points of the four converters are obtained via the following equations:

- **Power setting for the four converters:**  $P_1, P_2, P_3,$  and  $P_4$
- **Resistance of the four transmission lines:**  $R_{T1}, R_{T2}, R_{T3},$  and  $R_{T4}$

- **DC Voltage setting of the four Converters:**  $V_1, V_2, V_3,$  and  $V_4$

The unknown variables are:

- **Current of the four transmission lines:**  $I_{T1}, I_{T2}, I_{T3},$  and  $I_{T4}$ . The current directions are shown in Fig. 2.6.

All the unknown variables can be determined using Kirchhoff's Current Law (KCL) and Kirchhoff's Voltage Law (KVL). In this test system, the power loss ratio is about 4%, which means  $P_1 + P_4 = 1.04(P_2 + P_3)$ .

$$\begin{cases} V_2 = V_1 - I_{T1}R_{T1} \\ V_3 = V_1 - I_{T4}R_{T4} \\ V_2 + I_{T2}R_{T2} = V_3 + I_{T3}R_{T3} = V_4 \\ P_1 = V_1(I_{T1} + I_{T4}) \\ P_2 = V_2(I_{T1} + I_{T2}) \\ P_3 = V_3(I_{T3} + I_{T4}) \\ P_4 = V_4(I_{T2} + I_{T3}) \end{cases} \quad (2.7)$$

There are seven unknown variables and seven independent equations. With the right DC voltage settings, the desirable power flow pattern is achieved. Based on the above formulations, operating three or four converters in DC voltage control mode is feasible. However, when the power flow of one converter changes, DC voltage-controlled converters will encounter power changes, which requires the AC grids to be strong enough to withstand unexpected power flow changes. The converters which are connected to weak AC grids should be in real power control mode. If all the converters are in DC voltage control mode, the MTDC system will have a better tolerance to pole-to-ground faults.

### 2.3.4 Converter Built-in Protection Unit

Each converter in the two main test systems has a built-in protection unit, which monitors the DC side current of the converter arms. When the DC current magnitude exceeds twice the rated current for over 0.1 ms, the converter built-in protection unit will send a blocking signal to the converter and opens the AC circuit breaker on the AC side of the converter station (HB converter).

This protection unit protects the converter switches from over-current. The converter built-in protection is independent of the system-level fault detection and identification unit and therefore, it can be regarded as a backup protection unit. Therefore, the system-level and converter-level protection should detect the fault and isolate the faulted part before the converter built-in protection unit is triggered. The converter blocking delay is assumed to be 2 ms and the AC circuit breaker operating time is assumed to be 40 ms for both opening and closing.

### 2.3.5 High Voltage DCCBs

Using DCCBs to interrupt the DC fault current is one solution to protect the MTDC systems against DC faults. There are several types of DCCBs:

- **Semiconductor-based:** Similar to other electronic switches, semiconductor-based DCCBs have a very short interruption time. However, they have a high conduction loss during the normal operation [47].
- **Mechanical:** Mechanical DCCBs are slower than semiconductor-based DCCBs, but their conducting losses are negligible [48]. Mechanical circuit breakers usually come with resonant circuits, which provides an AC current during their operation. The AC current superimposed on the DC current creates a zero crossing in the main circuit breaker. The main circuit breaker is closed during normal operation and can only open near the zero crossing [49].
- **Hybrid:** Hybrid DCCBs consist of two or more parallel conduction branches [50]. In general, one branch is the main conducting branch and others are energy absorption branches [51]. The main conduction branch includes several semiconductor switches and an ultra-fast mechanical dis-connector. This helps to reduce the loss during normal operation. The other conduction branches, namely the main breaker branches, consist of a number of semiconductor switches. During the fault, the current will be transferred from the main conduction branch to the main breaker branches. The main breaker branches will interrupt the fault current. A hybrid DCCB employs a large number of electronic switches [52].
- **Modular:** The main breaker branch of a modular DCCB consists of a number of SMs. There are several structures for the SMs. The SMs can be similar to the above-mentioned hybrid DCCBs. A new submodule structure is proposed in [53]. The advantage of modular DCCBs is the flexibility of voltage and current ratings.

Different DCCB technologies are discussed in [54,55]. But, high voltage DCCBs are still immature and expensive for commercial implementation [23]. High voltage DCCBs that can interrupt large over-currents are out of the scope of this thesis. Mechanical DCCBs or mechanical disconnectors (MDs) are mature and cheap compared with hybrid high voltage DCCBs. But mechanical DCCBs can only work when the currents and voltages are below certain levels. The protection algorithm proposed in this thesis only employs mechanical DCCBs.

### 2.3.6 Backup Protection

Backup protection should be considered when planning an MTDC system. Backup relaying algorithms are discussed in [24]. Backup protection is vital when the primary protection fails. Backup protection can be divided into local and remote protections. There are

two failures that may happen to the primary protection system, which can be taken care of by the backup protection system.

- **Breaker failure:** When a fault is detected by the primary relay, the associated breaker should open and interrupt the fault current. If the current is still higher than a threshold after breaker interruption time, a breaker failure signal should be sent to open the adjacent breakers, isolating the fault and the failed breaker. Normally, there is no duplication of the primary breaker on the same line in one converter station [56].
- **Primary relay failure:** When a fault occurs, if the primary relay fails to detect the fault and send a signal to the breaker after a certain period, there should be a second relay to detect the fault and trip the breaker. The two relays should use different fault detection methods and use individual communication method to send a signal to the breaker.

Remote backup protection works when the fault cannot be cleared by local backup protection. When the primary protection fails to interrupt the fault current, the fault current may flow to the adjacent stations. In this case, the protection system of the adjacent stations must interrupt the fault current. In case of an MTDC system, if blocking the converter and opening the ACCBs fail to interrupt the fault current, remote AC sources which feed the MTDC system should be disconnected, i.e., the backup protection of AC system should operate.

## 2.4 Summary

In this chapter, the modeling of MMC-VSCs and MTDC systems and several important technologies related to the MTDC system protection are discussed. Two test systems are introduced for fault transient response and protection algorithm studies. The four-level controllers for MTDC systems are introduced. In fault situations, each level of the controller has individual responsibilities. Defining the responsibilities of each controller during the fault is important for designing a reliable and efficient fault detection and protection algorithm.

# 3

## Fault Transient Response of Hybrid DC Systems

### 3.1 Introduction

A hybrid MTDC system consists of different types of converters in one system and the fault transient is a combination of those of different converters. Fault transient study is the key to determine the required protection procedures. The converter-type and system configuration are the two main factors that influence the system fault transient responses. In this chapter, first, the fault transient study of the point-to-point HVDC system is conducted. Second, the difference between the fault transients of FB and HB converters are identified. Third, the fault transient responses of the hybrid MTDC systems are studied. For an MTDC system, AC side faults are not as severe as DC side faults. When an AC side fault occurs, the DC current will not be as high as the case, where a DC fault occurs, although the stable operation of the system would be interrupted. This thesis focuses on the protection of DC side faults. There are three main types of DC faults:

- Pole-to-pole,
- Pole-to-pole-to-ground, and
- Pole-to-ground.

In all the simulations, pole-to-pole-to-ground faults have similar fault transients to pole-to-pole faults. The grounding of fault impedance allows the energy in the DC grid to discharge faster. Therefore, in the rest of the thesis, only the study results for pole-to-pole and pole-to-ground faults are provided.

The fault transient is also influenced by the grounding type of the DC terminals of all the converters. In this thesis, high impedance grounding type is selected in all the test systems as it is the proper grounding type for symmetric, mono-polar MTDC systems [32]. With high impedance grounding, the midpoint voltage of the converter DC terminal is nonzero during pole-to-ground faults. The steady-state fault current for high impedance grounded converters are significantly smaller compared with low impedance grounded converters during pole-to-ground fault. Selecting high impedance grounding for all the converters reduces the impact of pole-to-ground faults. Pole-to-pole faults result in large over-currents and rapid DC voltage changes. Pole-to-ground faults result in smaller DC voltage and current oscillations, which would interrupt the stable system operation.

In [57], the fault transient of an MMC is divided into three stages:

- **Stage 1:** Discharge of cable and SM capacitors.
- **Stage 2:** Uncontrollable current flow from AC grid to DC system through anti-parallel diodes.
- **Stage 3:** Activation of ACCBs and isolation of converters from the AC grid.

During pole-to-pole faults, the three stages in a HB MMC are completed by two protective operations. The blocking of the HB converter occurs at the boundary of stages 1 and 2. The opening of the ACCB occurs at the boundary of stages 2 and 3. In a FB MMC, the anti-parallel diodes do not allow the AC grid to feed the DC system when the converter is blocked. So, stage 2 does not exist in the FB converter fault transient. The boundary between stage 1 and stage 3 is the converter blocking. In all the fault transient tests, the converter built-in protection unit is the only protection for the converters. In HB converters, the ACCBs will open after blocking the converters. During pole-to-ground faults, there is no clear boundary between the stages. The discharge of cable and SM capacitors occurs as the DC voltage is lower than the operating voltage, where the uncontrollable current flow through anti-parallel diodes also occurs. So, the three stages are only distinguishable during pole-to-pole faults.

### 3.2 Pole-to-Pole Fault Transients

In all the pole-to-pole fault scenarios, the fault is applied in the middle of one transmission line. Pole-to-pole faults cause large over-currents at the DC side of converters, which trigger the converter built-in protection unit. After detecting the fault, protective operations should be taken to interrupt the fault current. Blocking the converters is a necessary step to prevent any damage to the electronic switches and to prevent the discharge of the converter SM capacitors to the fault. In all the pole-to-pole fault simulations, the fault duration is 200 ms to reveal the fault transient in the three stages.

### 3.2.1 Fault Transient Response of the Point-to-Point Hybrid HVDC System

The simplest hybrid test system is the point-to-point HVDC system with one FB converter and one HB converter. The fault transient of the system is the combination of those of FB and HB converters. In the point-to-point HVDC test system of Fig. 2.5, Converter 1 is a FB MMC and Converter 2 is a HB MMC. The fault impedance is  $1 \Omega$ . The waveforms of DC current, DC voltage, and AC current are analyzed in the three discussed stages, respectively. The timeline and stages of the fault transient are shown in Fig. 3.1.

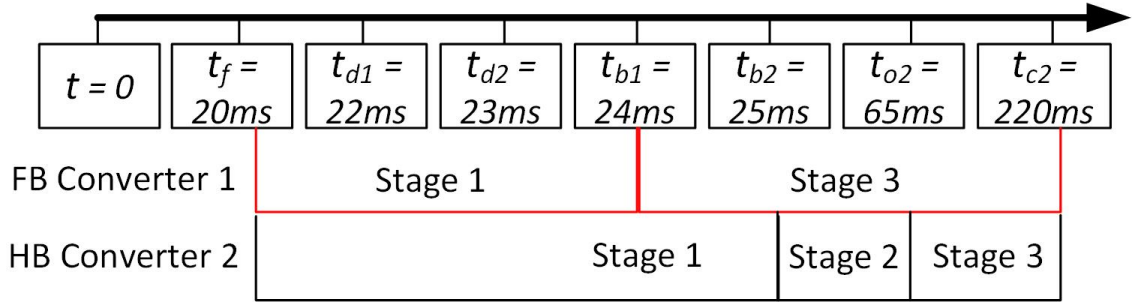


Figure 3.1: Timeline and stages of the pole-to-pole fault transient of the hybrid point-to-point HVDC system.

- $t_f$ : Fault instant,
- $t_{di}$ : Fault detection instant of Converter  $i$ ,
- $t_{bi}$ : Blocking instant of converter station  $i$ ,
- $t_{oi}$ : ACCB opening instant of converter station  $i$ ,
- $t_c$ : Fault clearing instant,  $t_c = t_f + \text{Fault duration}$ ,

The DC current waveforms of converters are shown in Fig. 3.2. The two converters show the same fault transients during stage 1. Although the two converters are at the same distance from the fault, their fault detection instants are different. During the steady-state operation, the DC current of Converter 1 and Converter 2 are 1.6 kA and -1.6 kA, respectively. When the fault occurs, the current direction of Converter 2 changes and the current increases from -1.6 kA to 4 kA to trigger the converter built-in protection unit. While the current of Converter 1 increases from 1.6 kA to 4 kA to trigger the same current threshold. The current rate of change for the two converters during the fault is the same in this simulation. The current rate of change is associated with the fault impedance, fault distance and transmission line parameters. So, Converter 2 detects the fault 1 ms after Converter 1.

The DC side currents of the two converters rise up to over three times the rated value. There are several factors that influence the current magnitude during stage 1, including:

- **Operating voltage:** The higher the operating voltage, the larger the fault current.
- **Fault impedance:** The smaller the fault impedance, the larger the fault current.
- **Blocking delay:** The longer the blocking delay, the larger the fault current.

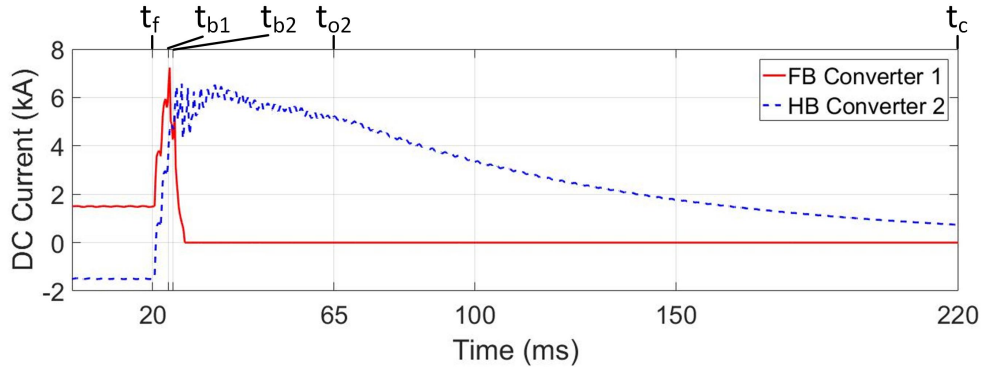


Figure 3.2: DC currents of the converters in the hybrid point-to-point HVDC system during the pole-to-pole fault.

When the pole-to-pole fault occurs in the system, the two AC sources are feeding the DC fault during stage 1. When the two converters are blocked at  $t = 24$  ms and  $t = 25$  ms, respectively, the fault transient of Converter 1 enters stage 3 while the fault transient of Converter 2 enters stage 2. The DC side current of Converter 1 drops to zero because FB converters can block any contribution from the AC side. The DC side current of Converter 2 remains at a high value. If the ACCB does not open, the fault current will reach a steady-state value of 3 kA at Converter 2 side. This current magnitude depends on AC source parameters and the current loop resistance. The current flow path during  $t = 24 - 65$  ms is shown in Fig. 3.3 (a). At  $t = 65$  ms, the fault transient of Converter 2 enters stage 3. The fault current drops down slowly. There is a closed current loop in the test system as shown in Fig. 3.3 (b). This current is referred to as the uncontrollable looping current in the rest of the thesis. The energy in the DC grid will be dissipated through the fault resistance and MMC inner resistance. Eventually, the fault currents of the two converters become zero. The current flow through the fault impedance is shown in Fig. 3.4. This current is the summation of the DC side currents of the two converters.

The DC voltage waveforms of the converters are shown in Fig. 3.5. During stage 1, the DC voltage of Converter 1 drops to zero and oscillates above zero. During stage 3, the DC side voltage drops to negative and oscillates around zero. The reason for this symmetrical oscillation after the blocking of Converter 1 is due to the traveling waves during the discharge of cable capacitors into the fault. The voltage oscillation frequency is 375 Hz because of the 200 km distance of the fault from the converter terminal. The wave travels forward and backward on both positive and negative pole. In one cycle, the traveling

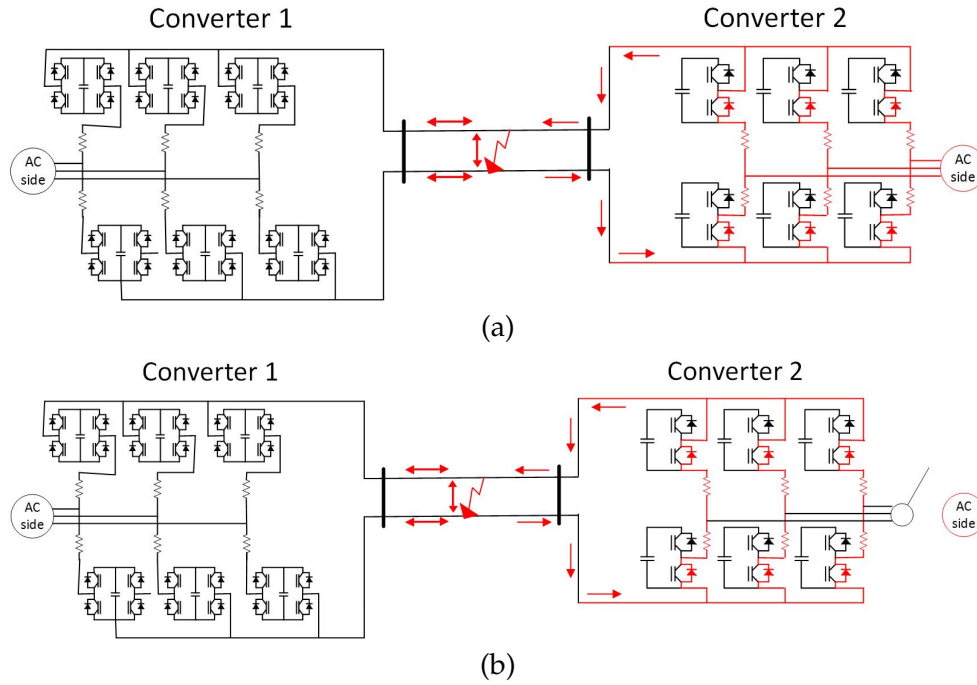


Figure 3.3: Current flow path during: (a) stage 2 and (b) stage 3.

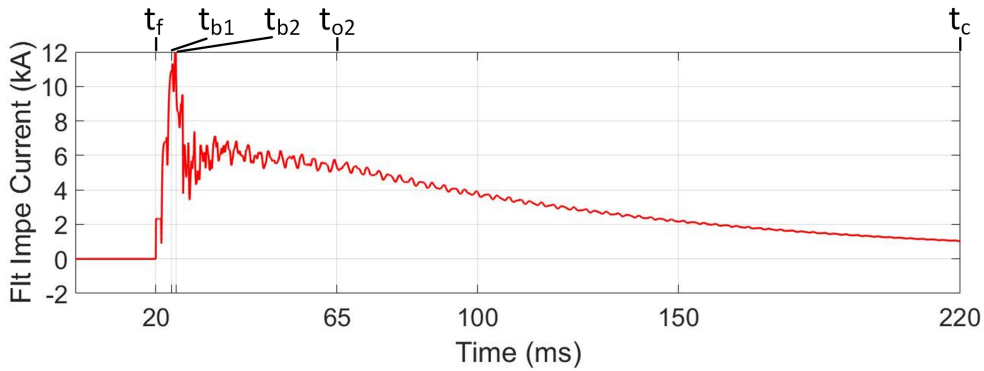


Figure 3.4: Current flow through the fault impedance during the pole-to-pole fault.

distance of the wave is four times the distance of the fault from the converter terminal. In a point-to-point HVDC system, the voltage oscillation frequency of a FB converter during the fault transient stage 3 is  $f_o$ , where

$$\frac{1}{f_o} = \frac{4 * \text{fault distance}}{300,000 \text{ km/s}} \tag{3.1}$$

These oscillations will continue until the energy of the DC side is dissipated in the current loop resistance. For an HVDC system with only HB converters, the DC terminal voltage is always positive during stages 2 and 3 because the fault current flow is unidirectional as shown in Fig. 3.2. The DC terminal voltage of Converter 2 in the hybrid point-to-

point HVDC system shows some oscillation during stages 2 and 3 due to the influence of Converter 1, as shown in Fig. 3.5.

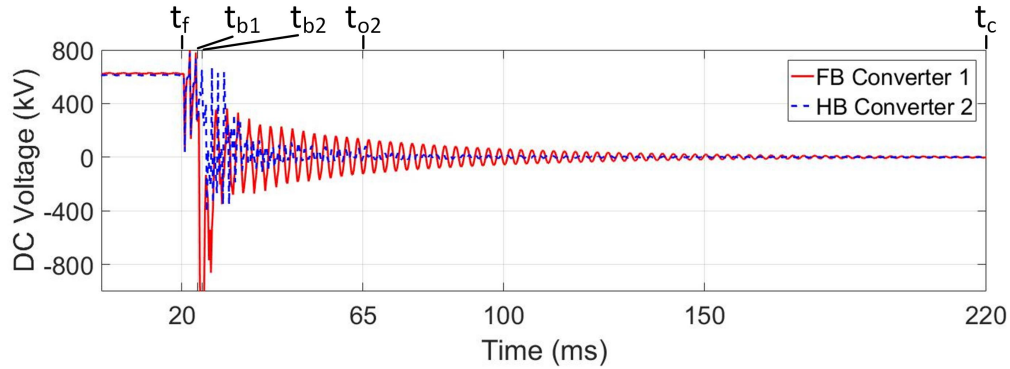


Figure 3.5: DC voltages of converters in the hybrid point-to-point HVDC system during the pole-to-pole fault.

The currents of the two AC sources are shown in Fig. 3.6. The AC source of Converter 1 feeds the DC fault during stage 1. When Converter 1 is blocked at  $t = 24$  ms, the AC source current drops to zero. The AC source of Converter 2 feeds the DC fault during stages 1 and 2. The opening of the ACCB interrupts the AC side contribution to the fault current at  $t = 65$  ms.

To study the impact of fault impedance value on the fault transient responses of a hybrid point-to-point HVDC system, two fault transient tests are conducted with  $10 \Omega$  and  $20 \Omega$  fault impedances, respectively. The rest of the parameters are the same as the previous studies. The simulation results show that the voltage and AC current waveforms are identical to the former fault scenario, where the fault impedance is  $1 \Omega$ . However, the DC current magnitude of Converter 2 is different as shown in Fig. 3.7. For a larger fault impedance, the fault currents in stages 1 - 3 will be smaller. Therefore, the activation of the converter built-in protection unit will be delayed. A larger fault impedance also allows for a faster discharge of the DC grid. For a larger fault impedance (e.g.  $100 \Omega$ ), the converter built-in protection unit will not be triggered by the fault.

### 3.2.2 Fault Transient Response of the Point-to-Point HVDC System with FB Converters

In the point-to-point HVDC test system with either FB or HB SMs, the pole-to-pole fault transients are similar to the performance of individual converters in a hybrid point-to-point HVDC system. The timelines of the fault transient is similar to the previous study in the hybrid HVDC system as shown in Fig. 3.8. The fault transient of FB converters in a point-to-point HVDC system is shown in Fig. 3.9. The DC side voltage oscillates symmetrically after blocking the converters. The DC side current rises up to several times

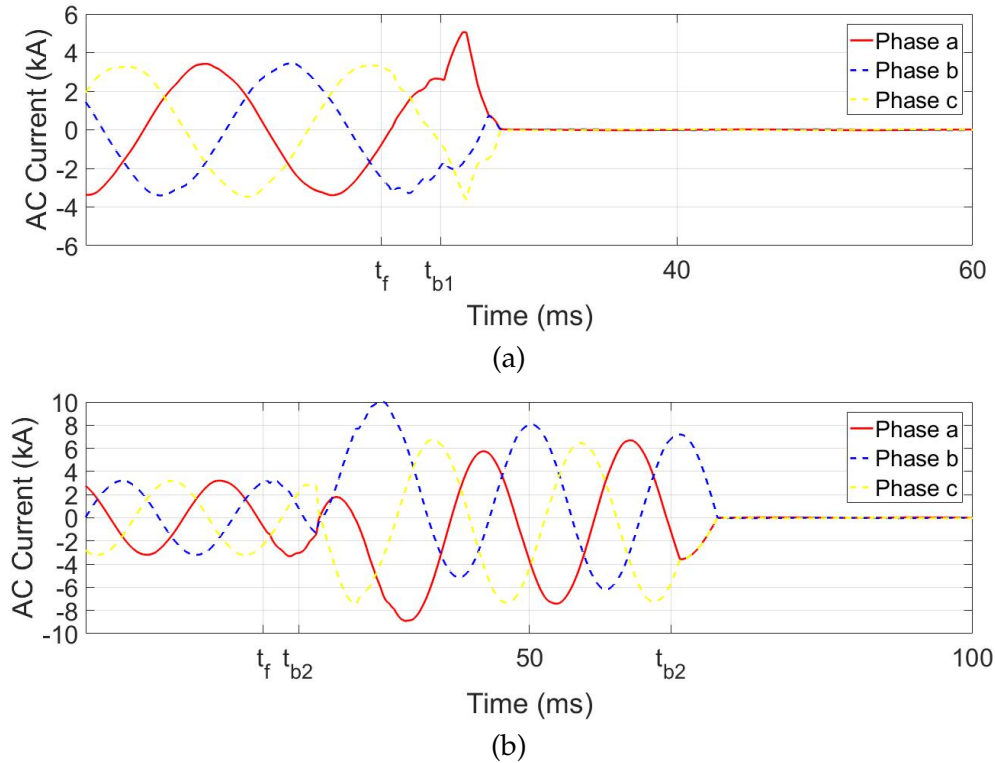


Figure 3.6: Hybrid point-to-point HVDC system AC side current during the pole-to-pole fault for (a) AC source 1 and (b) AC source 2.

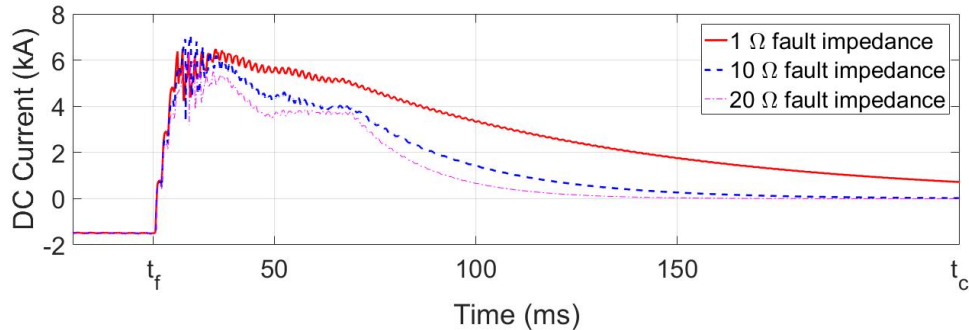


Figure 3.7: DC current of HB Converter 2 for various fault impedances.

the rated current during stage 1 and drops to zero during stage 3. The AC sources feed the DC fault only during stage 1.

### 3.2.3 Fault Transient Response of the Point-to-Point HVDC System with HB Converters

The timeline and stages of the pole-to-pole fault transients of the point-to-point HVDC test system with only HB converters is shown in Fig. 3.10 and the results are shown in Fig. 3.11. The current waveform shows the boundary between stages 2 and 3. In stage 2,

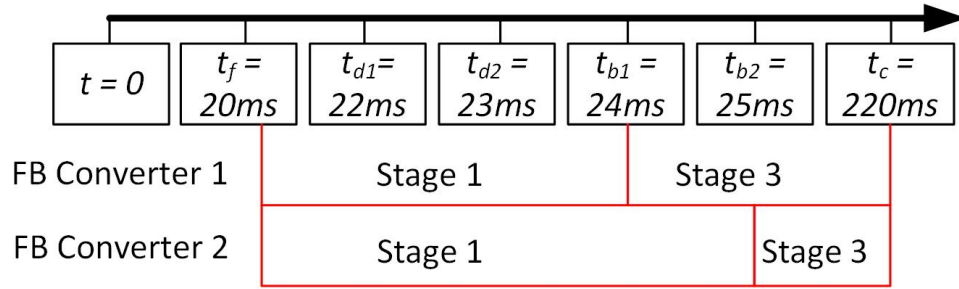
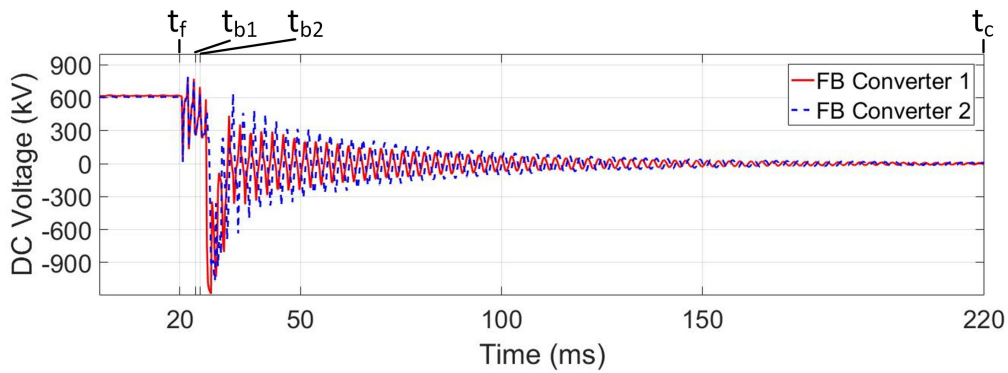
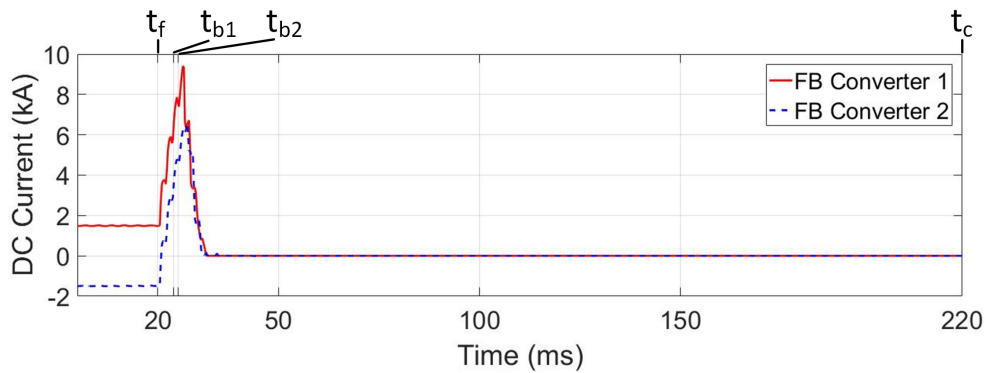


Figure 3.8: Timeline and stages of the pole-to-pole fault transient of the FB point-to-point HVDC system.



(a)



(b)

Figure 3.9: Pole-to-pole fault transient of the point-to-point HVDC system with FB converters: (a) DC voltage of Converter 1 and Converter 2 and (b) DC current of Converter 1 and Converter 2.

the AC sources are feeding the DC fault, resulting in a six-pulse waveform superimposed on the stage 3 transient current. The DC voltage waveform in stage 2 is also influenced by the AC sources.

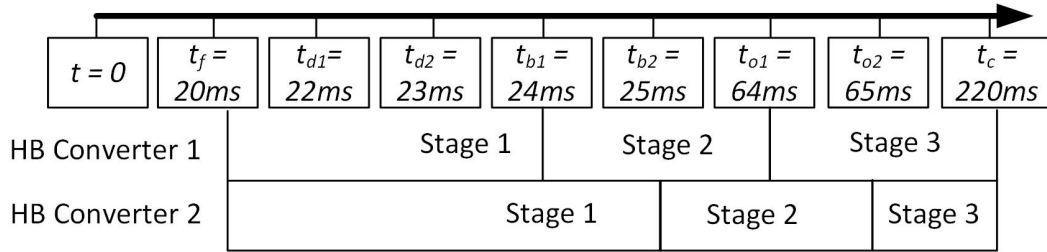


Figure 3.10: Timeline and stages of the pole-to-pole fault transient of the HB point-to-point HVDC system.

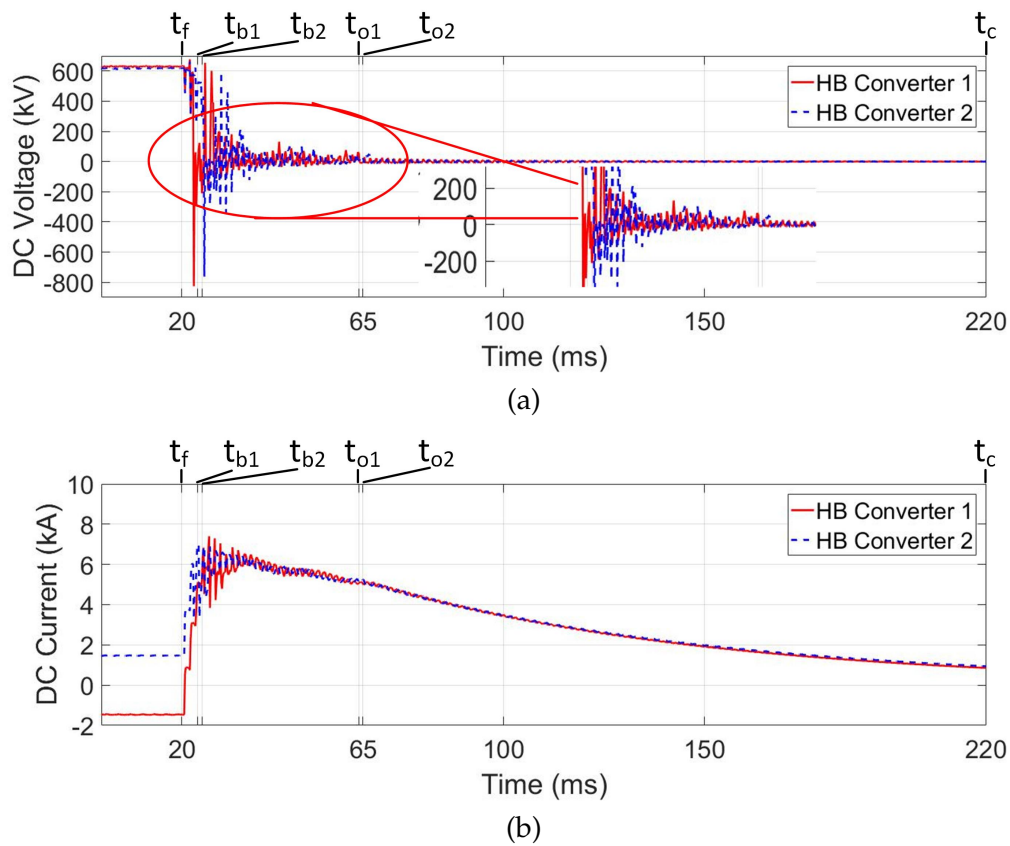


Figure 3.11: Pole-to-pole fault transient of the point-to-point HVDC system with HB converters: (a) DC voltage of Converter 1 and Converter 2 and (b) DC current of Converter 1 and Converter 2.

### 3.2.4 Fault Transient Response of the Hybrid Four-Terminal MTDC System

The fault transients of the hybrid four-terminal MTDC system, which contains different types of converters are studied in this section. In the hybrid MTDC system 2, only Converter 1 has FB SMs and the rest of the converters have HB SMs. The fault occurs on the middle of the T-line 3 and the fault impedance is  $1 \Omega$ . The fault transient response of the system is similar to that of the hybrid point-to-point HVDC system. The main difference

is that the energy in the MTDC system is discharged faster than the point-to-point HVDC system because there are several paths for the uncontrollable looping current and energy dissipation.

In an MTDC system with built-in protection unit for converters, the converter which is closer to the pole-to-pole fault would be influenced first. The current change rate during stage 1 depends on the impedance between the fault and the converter. A longer distance between the converter and the fault impedance results in a larger impedance, which leads to a smaller current rise rate. Therefore, the built-in protection unit of a distant converter will be triggered later than those converters, which are closer to the fault.

Converter 3 and Converter 4 are located at equal distances from the fault. However, the built-in protection of Converter 4 is activated earlier than Converter 3 because Converter 4 injects power to the DC side during normal operation while Converter 3 absorbs power from the DC side. During normal operation, the current of Converter 3 and Converter 4 are -1.6 kA and 1.6 kA, respectively. During the pole-to-pole fault, the current of Converter 4 increases 2.4 kA and triggers the built-in protection unit with a 4 kA current threshold while the current of Converter 3 increases 5.6 kA and triggers the same current threshold. With the same rate of current rise, the built-in protection unit in Converter 4 is activated 2 ms earlier than Converter 3.

The pole-to-pole fault transient timeline of the four-terminal MTDC system is shown in Fig. 3.12. The DC current waveforms are shown in Fig. 3.13. The converter built-in protection units of the converters 1-4 are triggered at 13 ms, 15 ms, 3 ms and 1 ms after the fault instant, respectively. The DC current waveform of Converter 3 shows a larger magnitude during stage 2 compared with that of stage 1. After the blocking of Converter 3, Converter 1 is still feeding the fault. When Converter 1 is blocked at  $t = 35$  ms, the fault current cannot flow through Converter 1, instead, the current flows through the diodes in Converter 3.

The voltage waveforms of the four converters are shown in Fig. 3.14. In the pole-to-pole fault transient response of the hybrid point-to-point HVDC test system, the DC voltages of Converter 1 and Converter 2 are almost independent from each other. In the hybrid four-terminal test system, there are two transmission lines connected to every converter. Therefore, the DC voltages of all the converters are influenced by the current contribution from the other converters. The voltage of Converter 1 is not a symmetric oscillation because of the influence of other converters.

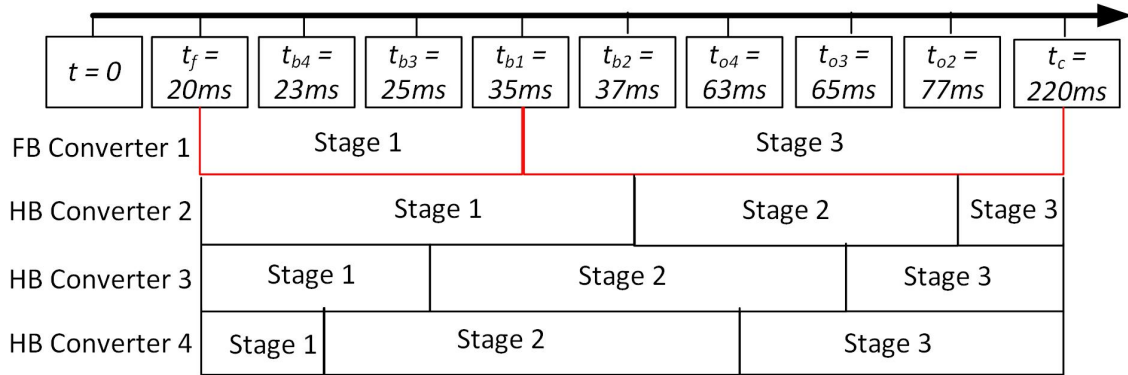
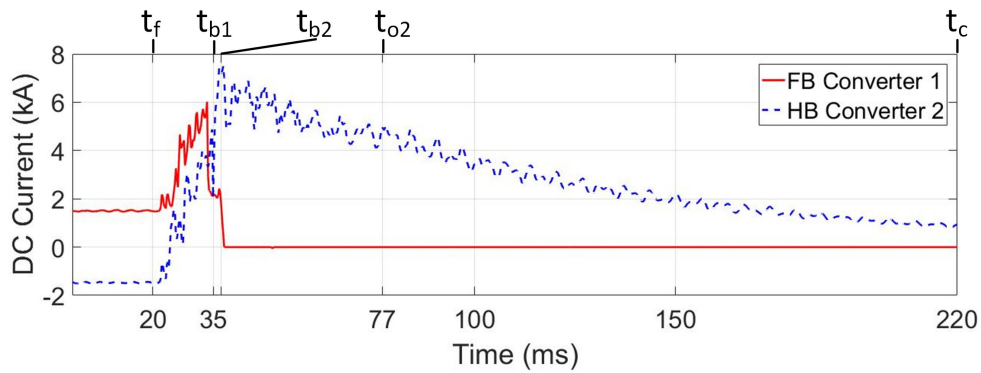
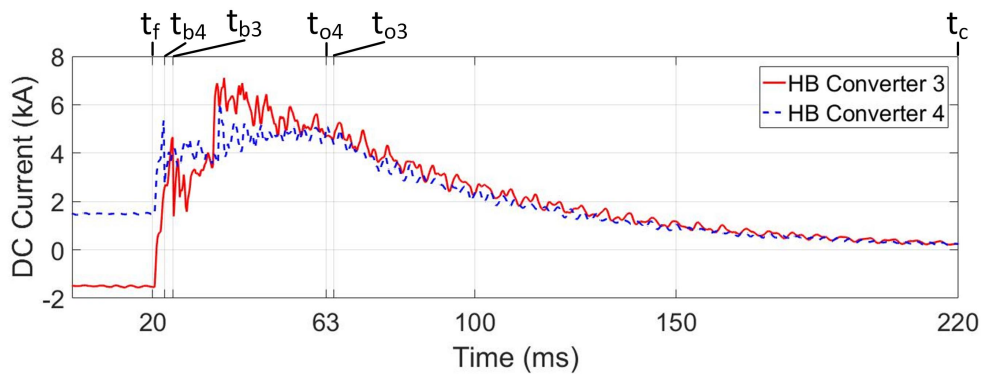


Figure 3.12: Timeline and stages of the pole-to-pole fault transient of the hybrid four-terminal MTDC system.



(a)



(b)

Figure 3.13: Pole-to-pole fault transient of the hybrid MTDC system: (a) DC current of Converter 1 and Converter 2 and (b) DC current of Converter 3 and Converter 4.

### 3.3 Pole-to-Ground Fault Transients

In this section, first, the pole-to-ground fault transient of the point-to-point HVDC test system with either two FB converters or two HB converters is studied. Second, pole-to-ground fault transient of the four-terminal test system is studied. The only protection of

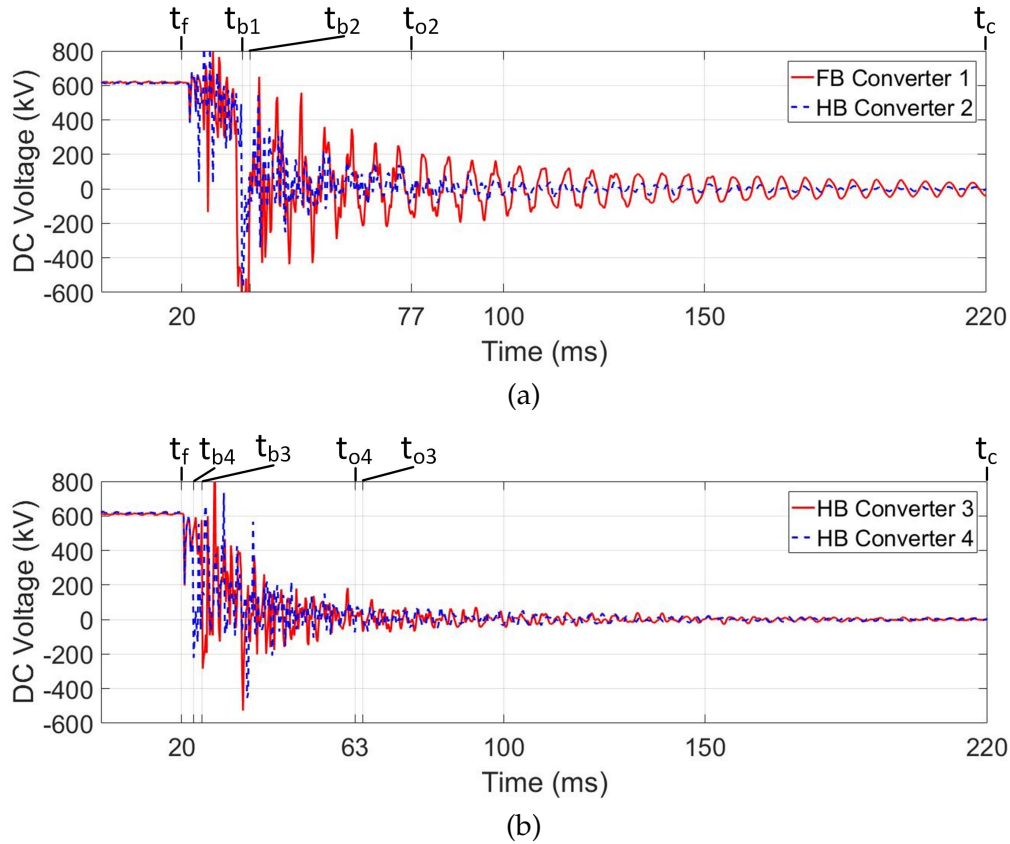


Figure 3.14: Pole-to-pole fault transient of the hybrid MTDC system: (a) DC voltage of Converter 1 and Converter 2 and (b) DC voltage of Converter 3 and Converter 4.

the system is the built-in protection unit in every converter with a 4 kA current threshold. During pole-to-ground faults, the point-to-point HVDC system will reach a steady-state current, which does not activate the converter built-in protection unit. In the point-to-point HVDC system, the fault duration is assumed to be 1 s. In the hybrid four-terminal MTDC system, first, a temporary fault with a duration of 0.5 s is applied to the system. This fault does not activate the converter built-in protection unit. Second, a temporary fault with a duration of 1 s is applied to the system. Such a fault will activate the converter built-in protection unit.

### 3.3.1 FB and HB Converter Comparison

The pole-to-ground fault responses of FB and HB converters are different. In the point-to-point HVDC test system, the fault is applied at  $t = 20$  ms to the midpoint of the positive pole of the transmission line. The timeline of the fault transient response of the FB and HB point-to-point HVDC systems is shown in Fig. 3.15. The fault duration is 1 s and the fault impedance is  $1 \Omega$ . The simulation results for FB and HB configurations are compared and are shown in Figs. 3.16 and 3.17.

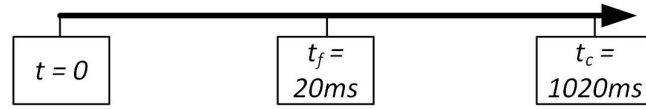


Figure 3.15: Timeline of the pole-to-ground fault transient of FB and HB point-to-point HVDC system.

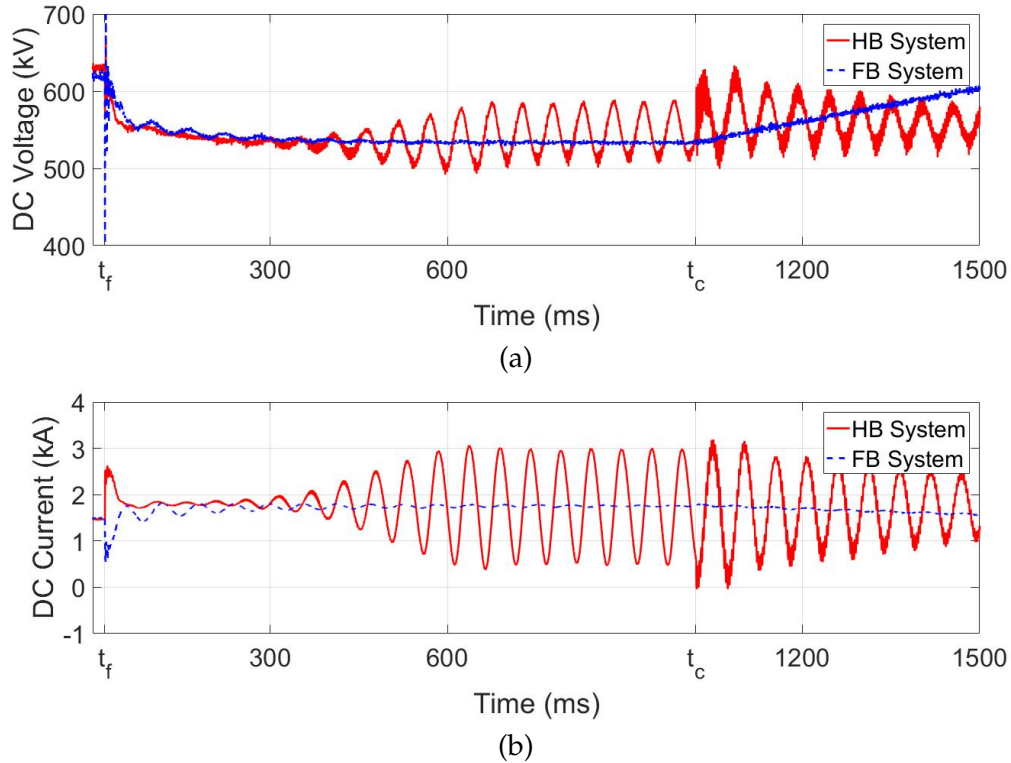


Figure 3.16: Pole-to-ground fault transient of the FB and HB point-to-point HVDC system. (a) DC voltage and (b) DC current.

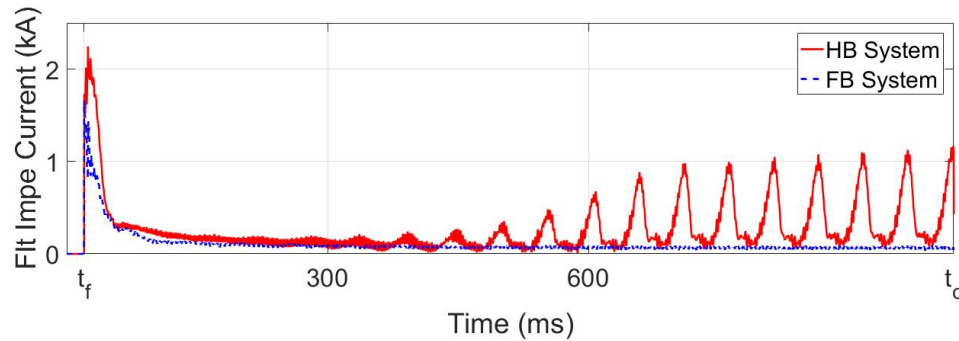


Figure 3.17: Current flow through fault impedance during the pole-to-ground fault.

As shown in Figs. 3.16 and 3.17, both systems encountered oscillations in the DC voltage and current when the fault is applied and cleared. But the current is not high enough

to trigger the converter built-in protection unit. In the FB converter, due to the transformer grounding (grounded Y/ $\Delta$ ), the steady-state current flow through the fault impedance is near zero. During the normal operation, the positive and the negative pole voltages are 320 kV and -320 kV, respectively. During the fault, the positive pole voltage drops to about zero and the negative pole voltage drops to about -550 kV. The reason for this lower DC terminal voltage during the pole-to-ground fault is that the current flow from the negative DC terminal through the grounding resistor increases compared with the normal operation conditions. This effect influences both systems with HB and FB converters.

The pole-to-ground fault does not have a significant impact on the FB converters, while that is not the case with the HB converters. In the point-to-point HVDC system with two HB converters, the DC voltage and current waveforms show large oscillations. The current is not high enough to trigger the converter built-in protection unit. However, the stable operation of the system is interrupted. The current flow through the HB converters are shown in Fig. 3.16 (b). The current oscillation is caused by the current contribution from the AC grid through the anti-parallel diodes. During the pole-to-ground fault, the system with HB converters encounters a lower DC terminal voltage similar to the system with FB converters, lower than two times the line-to-neutral voltage of the AC grid (604 kV). Therefore, the AC grid will feed the DC grid through the diodes. This current injection flows to the ground through the fault impedance and makes the DC terminal voltage increase until the AC side cannot feed the DC grid anymore.

In the HB point-to-point HVDC system, the ACCB of Converter 2 is closed and the DC voltage is shown in Fig. 3.18. The AC source contribution to the DC grid through the diodes reaches a peak voltage of over 604 kV and steady-state voltage of 510 kV. So, when the DC terminal voltage of a HB converter is lower than 604 kV, the AC source will feed the DC grid through diodes. When the DC terminal voltage of a HB converter is lower than 510 kV, the current through the diodes is significantly larger.

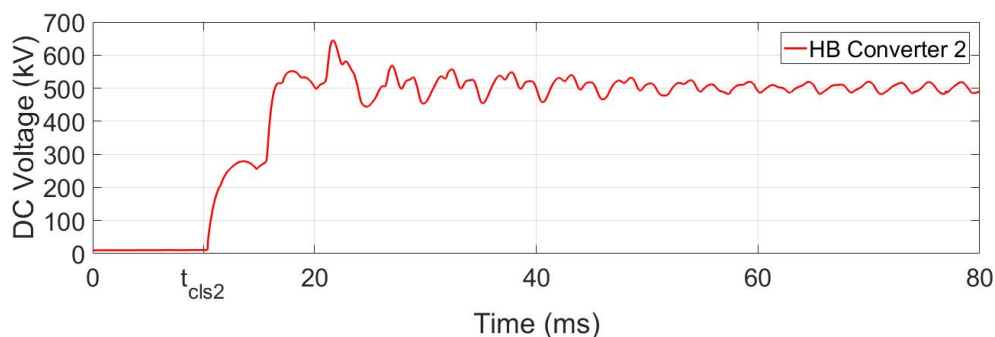


Figure 3.18: DC terminal voltage of Converter 2 caused by the uncontrollable AC source contribution.

As the current through the grounding resistor increases, the DC terminal voltage further decreases. This will result in an increase in the current flowing through the diodes, interrupting the steady-state operation as shown in Fig. 3.16(a) and (b). The voltage waveform in Fig. 3.16(a) shows that the system with HB converters cannot automatically restore its steady-state operation after the fault is cleared.

### 3.3.2 Fault Transient Response of the Hybrid Point-to-Point HVDC System

In the hybrid point-to-point HVDC system with both FB and HB converters, the pole-to-ground fault transient is a combination of FB and HB converter fault transients. A pole-to-ground fault is applied to the hybrid point-to-point HVDC test system where Converter 1 and Converter 2 have FB and HB SMs, respectively. Converter 1 is in DC voltage control mode and Converter 2 is in real power control mode. The timeline of the pole-to-ground fault transient responses are shown in Fig. 3.19. The DC side voltage and current waveforms are shown in Fig. 3.20. The current flow through the fault impedance is shown in Fig. 3.21.

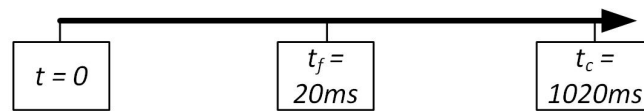


Figure 3.19: Timeline of the pole-to-ground fault transient of the hybrid point-to-point HVDC system.

As shown in Fig. 3.20 and 3.21, the hybrid point-to-point HVDC system can withstand the temporary pole-to-ground fault, although there will be some current and voltage oscillations in the system during the fault. The oscillations become more obvious after  $t = 450$  ms because the DC voltage is lower than 510 kV. The current flow through the fault impedance will reach a certain steady-state value in the end. This steady-state fault current value depends on the transmission line parameters and fault impedance. If the fault impedance is small enough, the fault current will be high enough to reach the current threshold of the built-in protection unit. After clearing the fault, the system can restore the steady-state operation automatically. Similar results have been obtained for the hybrid test system, where Converter 1 and Converter 2 have HB and FB SMs, respectively.

### 3.3.3 Fault Transient Response of the Hybrid Four-Terminal MTDC System

In this section, the pole-to-ground fault transient responses of the hybrid MTDC system 1 with FB Converter 1 and Converter 4 and HB Converter 2 and Converter 3 are studied. The fault impedance is  $1 \Omega$  and the fault duration is 0.5 s. The timeline of the pole-to-ground fault transient of the hybrid MTDC system 1 is shown in Fig. 3.22. The current waveforms of all four converters are shown in Fig. 3.23.

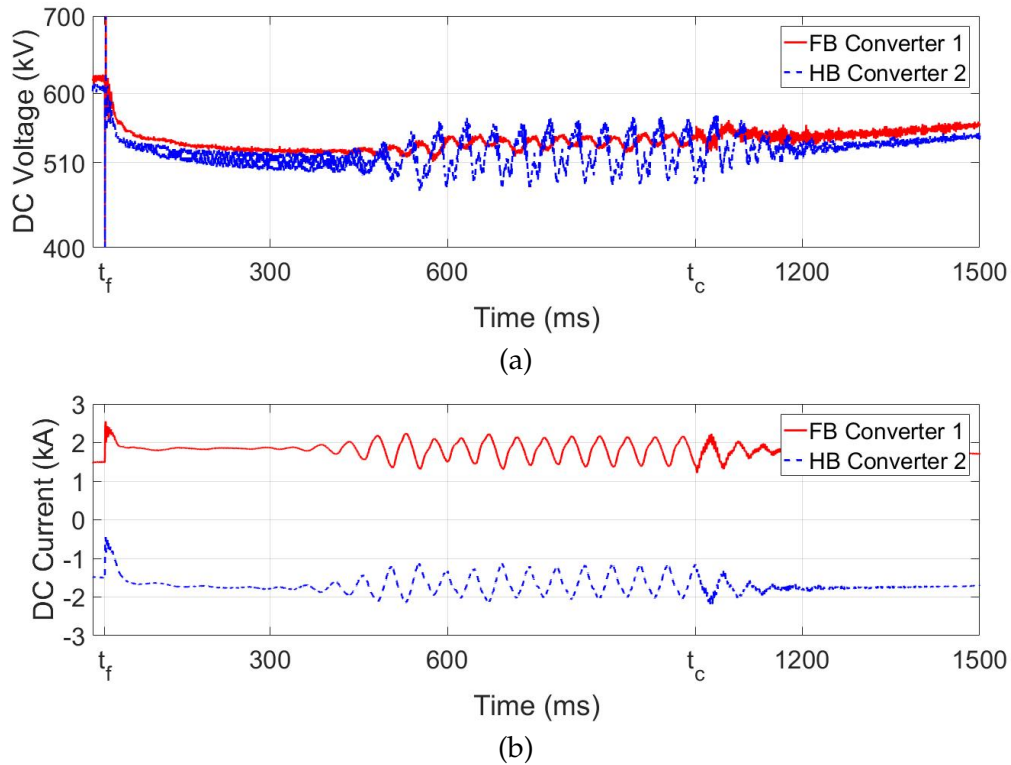


Figure 3.20: Pole-to-ground fault transient response of the hybrid point-to-point HVDC system: (a) DC voltage and (b) DC current.

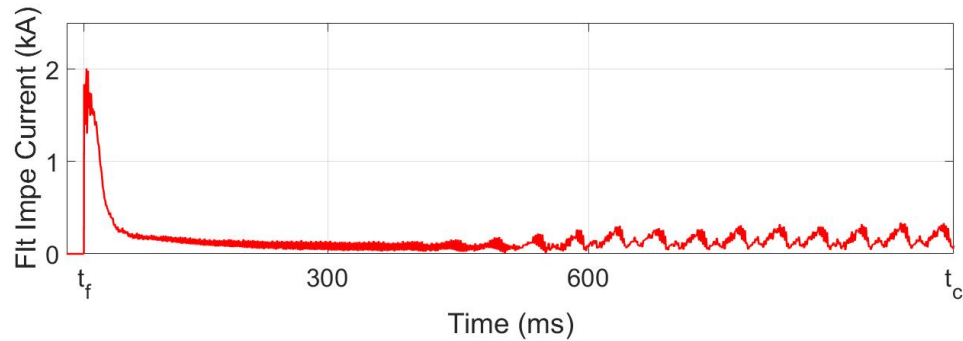


Figure 3.21: Fault impedance current during the pole-to-ground fault.

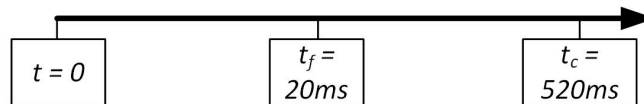


Figure 3.22: Timeline of the pole-to-ground fault transient of the hybrid MTDC system.

As shown in Fig. 3.23 and 3.24 (a), the pole-to-ground fault causes current oscillation as well as voltage oscillation in the MTDC test system. The voltage of Converter 3 and Converter 4 are similar to Converter 2 and Converter 1, respectively. The reason for the

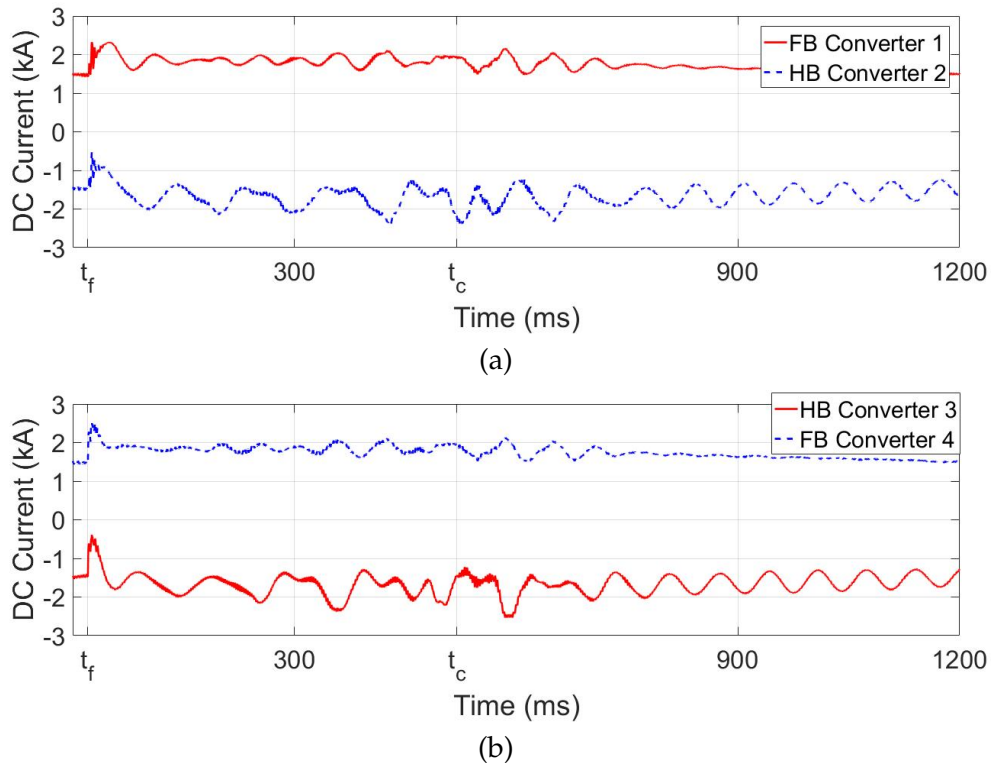


Figure 3.23: Pole-to-ground fault transient current: (a) Converter 1 and Converter 2 and (b) Converter 3 and Converter 4.

current oscillation is the uncontrollable AC source contribution through the HB converters (Converter 2 and Converter 3). However, the DC voltage of the system is higher than 510 kV during the fault and the current oscillation is not severe. When the fault is cleared, DC voltage-controlled converters (Converter 1 and Converter 4) can restore their stable operation. But, real power-controlled converters (Converter 2 and Converter 3) cannot maintain a stable DC terminal voltage, thus the current oscillations are sustained. The real power waveforms of Converter 3 and Converter 4 are shown in Fig. 3.24 (b). The power waveform of Converter 3 shows oscillations during the pole-to-ground fault. The energy loss during the fault is high, which is the difference between the power of Converter 3 and Converter 4. When the DC voltage is restored to 610 kV at  $t = 910$  ms, the AC source contribution through diodes is eliminated.

If the fault duration is longer than 0.5 s, the current oscillations will grow and eventually trigger the converter built-in protection unit. The timeline of a pole-to-ground fault study with a fault duration of 1 s is shown in Fig. 3.25. As shown in Fig. 3.26, in this fault scenario, the converter built-in protection unit is triggered at Converter 2 and Converter 3 at  $t = 970$  ms and  $t = 1005$  ms, respectively.

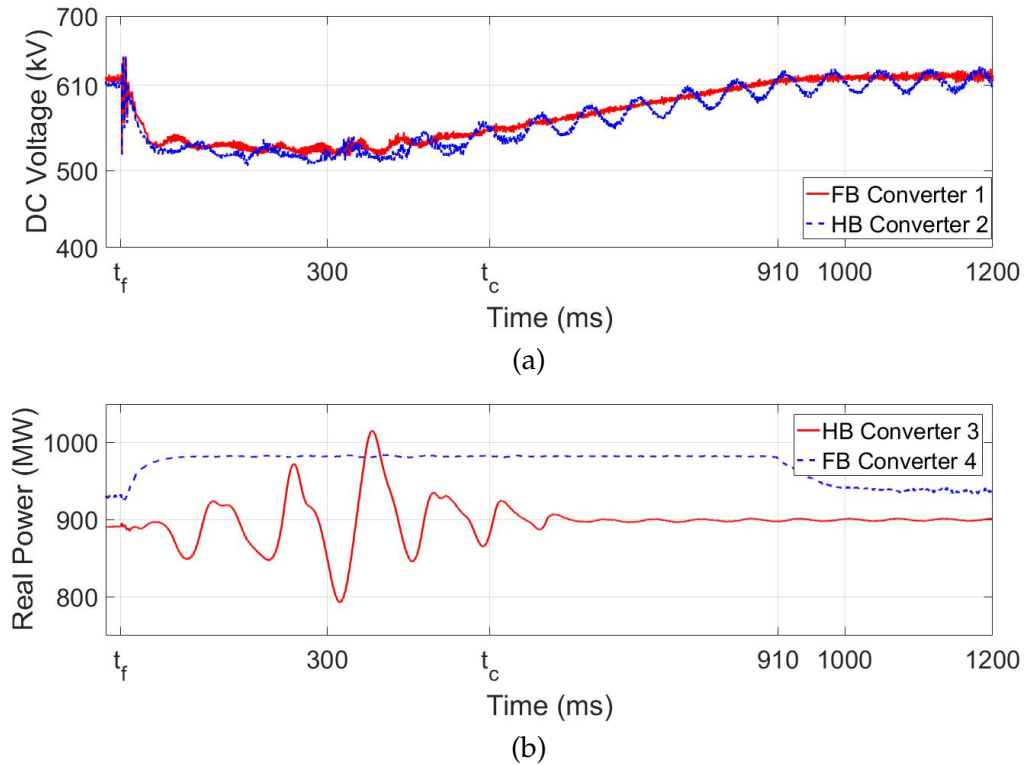


Figure 3.24: Pole-to-ground fault transient of the four-terminal MTDC system: (a) Voltage of Converter 1 and Converter 2 and (b) Real power of Converter 3 and Converter 4.

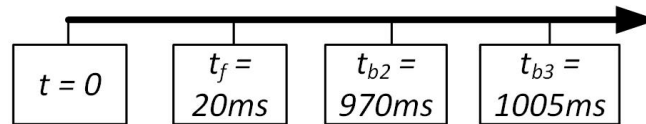


Figure 3.25: Timeline of the pole-to-ground fault transient of the hybrid MTDC system.

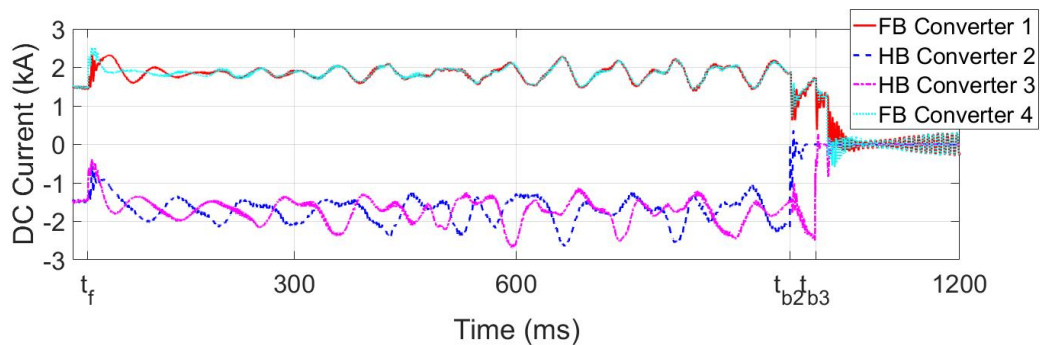


Figure 3.26: Pole-to-ground fault current of the four-terminal MTDC system.

To study the impact of the converter control modes on the fault transient responses of the hybrid MTDC system, Converter 1 and Converter 4 are changed to HB SMs and Con-

verter 2 and Converter 3 are changed to FB SMs. The control modes for the four converters are fixed in the MTDC test system. The simulation result shows that the system's capability to handle the pole-to-ground fault when HB converters are in charge of controlling the DC voltage is more limited compared with the case where FB converters maintain the DC voltage at a reference value. The uncontrollable looping current flowing through HB converters interrupts the DC voltage controllability of the converters faster. The converter built-in protection of Converter 2 and Converter 3 is triggered at  $t = 529$  ms and  $t = 555$  ms, respectively, as shown in Fig. 3.27. The current oscillations become larger and larger with time as shown in Fig. 3.28.

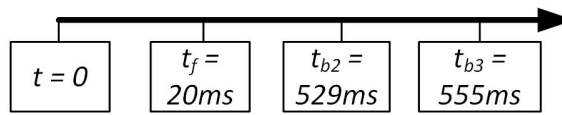


Figure 3.27: Timeline and of the pole-to-ground fault transient of the hybrid MTDC system.

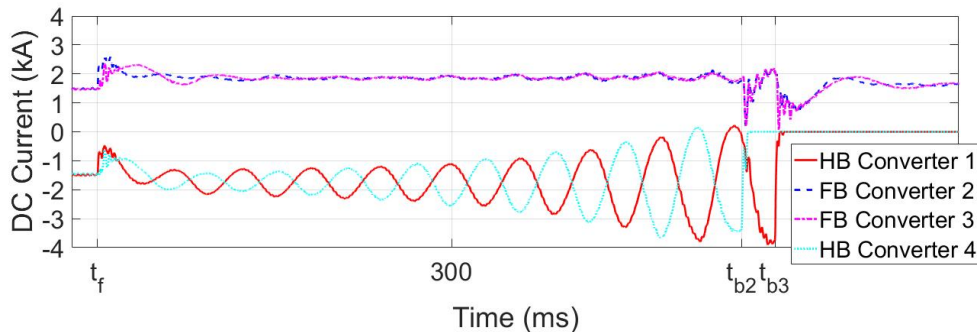


Figure 3.28: Pole-to-ground fault current of the four-terminal MTDC system.

### 3.4 Other Factors

There are two important factors influencing the fault transient response and the protection of a hybrid MTDC system:

- Fault impedance, and
- Converter blocking delay.

#### 3.4.1 Fault Impedance

The fault impedance directly influences the fault current magnitude. During pole-to-ground faults, a larger fault impedance current results in larger current oscillations. Therefore, a smaller fault impedance may result in an unstable MTDC grid. In the four-terminal test

system of this thesis, if a pole-to-ground fault impedance is  $8 \Omega$  or larger, the current oscillation will not trigger the converter built-in protection unit.

During pole-to-pole faults, a smaller fault impedance results in a higher current peak in stage 1 as well as a larger fault current magnitude after blocking the converter. Furthermore, a larger fault impedance results in a faster discharge of the energy in the DC grid, and consequently low voltage DC disconnecter can isolate the faulted line quickly. Overall, low impedance faults are more severe than the high impedance faults.

### 3.4.2 Converter Blocking Delay

The converter built-in protection unit does not rely on communication. However, fault detection, signal processing and disconnectors' operation require a certain time. The converter blocking time is assumed to be 2 ms in [38]. The converter blocking delay directly influences the fault current magnitude during stage 1. In the point-to-point HVDC test system, to find out the influence of converter blocking delay on converter SM capacitor voltages, the converter blocking delay is set to 2 ms and 3 ms, respectively. The total SM capacitors voltage of one converter arm for the two blocking delays is shown in Fig. 3.29.

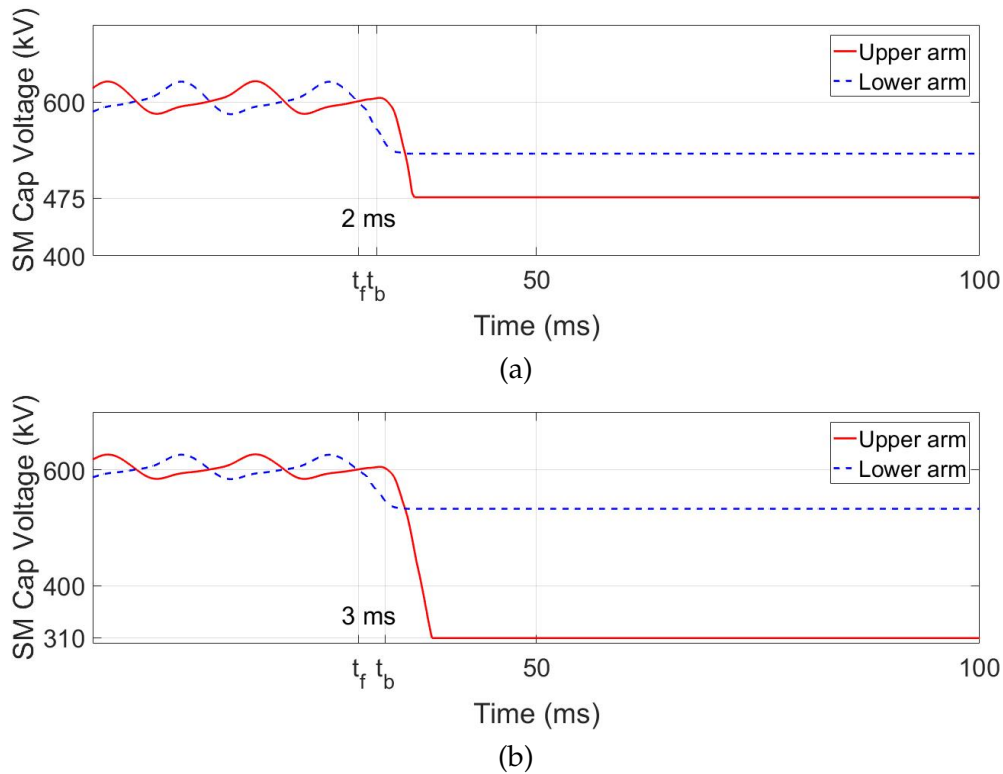


Figure 3.29: Total voltage of SMs in one arm: (a) Converter blocking delay of 2 ms and (b) Converter blocking delay of 3 ms.

As shown in Fig. 3.29, the upper arm and lower arm capacitors are discharged during the pole-to-pole fault. For both converter blocking delays, the lower arm capacitors were discharged to 530 kV. The upper arm capacitors were discharged to 475 kV and 310 kV when the converter blocking delay is 2 ms and 3 ms, respectively. The peak current of converter DC side is 20% higher when the converter blocking delay is 3 ms rather than 2 ms. Therefore, a fast fault detection and protection unit is vital for MTDC systems with large blocking delays.

### 3.5 Summary

In this chapter, the fault transient responses of the hybrid point-to-point HVDC and four-terminal MTDC systems during pole-to-pole and pole-to-ground faults are studied. The differences in the fault transient responses between FB and HB converters are associated with:

- **Pole-to-ground fault endurance:** FB converters have a better fault handling capability during pole-to-ground faults compared with HB converters.
- **Uncontrollable current flow through diodes:** When a DC fault occurs at the DC terminal of a HB converter, the DC voltage of the system will be lower than the rated voltage, which causes a current flow from AC source through the anti-parallel diodes of the HB converters, while FB converters have the ability to block bi-directional currents. The uncontrollable current flow through diodes is the main reason for the different fault transient responses of FB and HB converters.
- **Fault blocking capability:** When a DC fault occurs in an MTDC system, in a protection scheme which does not use DCCBs, the entire DC grid should be isolated and discharged. Blocking a FB converter can isolate the DC grid from the AC source. However, for a HB converter, isolating the DC grid from the AC grids requires the use of ACCBs.

When a pole-to-ground fault occurs in a hybrid MTDC system, the steady-state operation is interrupted. During the fault, the DC voltage of the entire DC grid will be lower than the rated voltage due to the current flow through the grounding impedance. For a real power-controlled converter, a lower voltage results in a higher current. Furthermore, the current contribution from the AC source affects the DC voltage-controlled converters, causing unstable DC voltages. An unstable DC voltage causes larger current oscillations in real power-controlled converters. This positive feedback will continue in the MTDC system until the converter built-in protection unit is triggered. Therefore, fault detection algorithms should quickly identify the abnormal current and voltage oscillations in an MTDC system and should use these measurements as one of the criteria to detect pole-to-ground faults. When a HB MMC is in charge of controlling the DC voltage, the oscillation

will grow as the DC voltage will be influenced faster by the uncontrollable looping current. A hybrid MTDC system cannot restore the stable operation automatically after the fault is cleared. When a pole-to-pole fault occurs in an MTDC system, all the converters are blocked to prevent damages to the switches. Therefore, a restoration algorithm is necessary after clearing or isolating the DC fault.

# 4

## Fault Detection, Isolation and System Restoration of Hybrid MTDC Systems

### 4.1 Fault Detection and Isolation

Understanding the fault transient is helpful for detecting a DC fault in an MTDC system. Based on the fault analyses of Chapter 3, the fault detection unit should use multiple inputs for DC fault detection. In the fault transient studies of the MTDC systems, voltage oscillations lead to current oscillations during pole-to-ground faults. During pole-to-pole faults, the DC voltage does not have a fixed pattern. However, the DC current during the fault increases unidirectionally. So, current derivative-based fault detection methods are more efficient and sensitive than voltage-based methods [58]. The converter built-in protection unit monitors the current magnitude to detect the fault. The proposed fault detection algorithm of this thesis relies on current derivative analysis. In a converter station, there are current sensors on all the transmission line terminals as well as the converter DC terminal. There are also DC disconnectors on the two ends of the transmission line, which are controlled by converter-level controllers. By monitoring the current of all current sensors, a converter-level controller should determine:

- Whether there is a DC fault in the MTDC system,
- Whether this fault is urgent, and
- What kind of protective action is needed.

In order to find out the answers to the questions, current waveforms from all current sensors should be monitored by converter-level controllers. Each converter-level controller

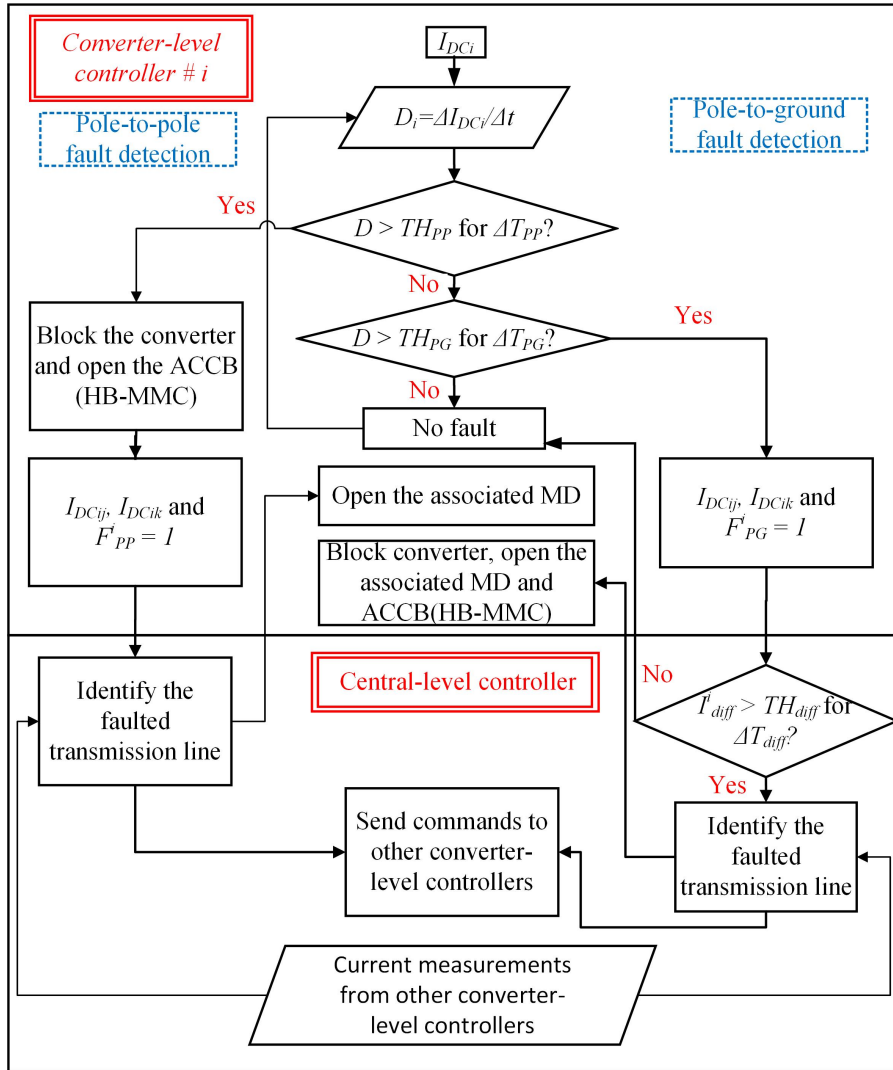


Figure 4.1: Fault detection and isolation algorithm.

monitors the current of its DC terminal. The fault detection and isolation algorithm is summarized in Fig. 4.1. This algorithm relies on the communications between the central-level controller and the converter-level controllers to block and protect the converters during pole-to-ground faults and to isolate the fault during both types of faults. In this algorithm, depending on the system scale, a delay of several tens of milliseconds can be expected. Based on the analysis of Chapter 3, during this delay, the pole-to-ground fault current does not increase beyond the first peak of the fault current and therefore does not result in any system damages. During pole-to-pole faults, converter-level controllers will block the converter without the command from the central-level controller, avoiding the communication delay.

In order to clear a DC fault without using DCCBs, discharging the entire HVDC grid

is necessary. Isolating the faulted transmission line by opening the MDs will enable the restoration of the healthy part of the grid. In the proposed algorithm, when the current derivative exceeds the pole-to-pole threshold ( $TH_{PP}$ ) for over a certain period ( $\Delta T_{PP}$ ), a pole-to-pole fault is recognized. When a pole-to-pole fault is detected, the converter-level controller blocks the converter immediately. Meanwhile, the central-level controller receives pole-to-pole fault flag ( $F_{PP} = 1$ ) and the current measurements from all the converter stations and identifies the faulted line based on the current directions. The central-level controller sends the necessary commands to the associated converter-level controllers to isolate the faulted transmission line when the DC voltage and current meet the requirements of the MDs. In the proposed algorithm, when the current derivative exceeds the pole-to-ground threshold ( $TH_{PG}$ ) for over a certain period ( $\Delta T_{PG}$ ), the converter-level controller sends a pole-to-ground fault flag ( $F_{PG} = 1$ ) to the central-level controller, which detects a pole-to-ground fault if the current difference between the two terminals of one transmission line is greater than a differential current threshold ( $TH_{diff}$ ). Upon fault detection, the central-level controller sends a blocking signal to all converter-level controllers and a trip signal to the associated converter-level controllers to open the MDs and isolate the faulted transmission line.

In the test system of this thesis, the pole-to-ground and pole-to-pole fault current derivative thresholds ( $TH_{PG}$  and  $TH_{PP}$ ) are selected to be 0.1 kA/ms and 1 kA/ms, respectively. The fault pick up times for pole-to-ground and pole-to-pole faults ( $\Delta T_{PG}$  and  $\Delta T_{PP}$ ) are selected to be 10 ms and 0.1 ms, respectively. If the current derivatives exceed the thresholds for less than 0.1 ms, no fault will be detected. The differential threshold ( $TH_{diff}$ ) is selected to be 50 A. The requirement for the opening of MDs is a current flow less than 50 A.

## 4.2 Restoration of HVDC Systems with FB or HB Converters

Pole-to-pole and pole-to-ground faults cause different fault transients in MTDC systems. In order to clear a DC fault without using high voltage DCCBs, discharging the entire DC grid is necessary in order to open the mechanical DC disconnectors. Isolating the faulted transmission line will enable the restoration of the rest of the MTDC system. The restoration algorithm of this thesis can be used to restore the system after the occurrence of all kinds of faults. When a DC fault occurs in an MTDC system, one transmission line is isolated in order to isolate the fault. The loss of one transmission line will change the current flows of the other transmission lines. However, as long as the thermal capacity of the transmission lines is not exceeded, all the converters can work at the pre-fault voltage and real power settings. If a converter is also lost with the faulted transmission line, the rest of the converters cannot operate at their pre-fault settings anymore. The loss of one or more converters requires the changes of voltage and power set-points of all the remaining

converters.

The restoration algorithm for FB converters is different from HB converters. As discussed, FB converters can block bidirectional currents while HB converters cannot. This difference results in different fault transient responses and also differences in the restoration algorithm. When the ACCB is closed after clearing the fault by opening the DC disconnectors, the currents from AC grids flow through the HB converters and energize the DC system. This uncontrollable current flow can be regarded as the small current injection test [28] to make sure the fault has been cleared.

#### 4.2.1 Restoration Algorithm of HVDC Systems with HB Converters

In case of an HVDC system with only HB-MMCs, opening the ACCBs is necessary to prevent the AC sources from feeding the DC fault. After clearing the fault, the ACCBs should be closed before restoring the converters. The AC source whose ACCB closes first after the fault will energize the DC system. The energization takes a certain period of time depending on the size of the DC grid. The blocked HB converter operates as a diode rectifier and the DC terminal voltage during this period is [59]:

$$V_{DC} = \frac{3\sqrt{3}}{\pi} V_m \approx 1.65V_m \quad (4.1)$$

where  $V_m$  is the amplitude of the AC phase voltage. In the test systems of this thesis, the steady-state DC terminal voltage reaches about 510 kV. The 510 kV DC voltage caused by the AC contribution through blocked HB converters is referred to as the AC peak voltage in the rest of the thesis. The restoration algorithm for HVDC systems with only HB converters has four steps:

- Step 1: The ACCB that is connected to a strong AC grid is closed.
- Step 2: After a short period (typically several milliseconds), when the DC voltage is stable and has reached the voltage threshold  $V_{TH1}$ , e.g. 90% of the AC peak voltage, all other ACCBs are closed.
- Step 3: When the DC voltage exceeds to  $V_{TH2}$ , e.g. 95% of the AC peak voltage, for  $\Delta T_2$ , e.g., 50 ms, all the DC voltage-controlled converters are deblocked one after another.
- Step 4: When the DC voltage exceeds to  $V_{TH3}$ , e.g., 95% of the rated DC voltage, for  $\Delta T_3$ , e.g., 20 ms, the remaining converters, which control the real power, are deblocked one after another.

For a point-to-point HVDC system, the delay time  $V_{TH3}$  before restoring the real power-controlled converters can be as short as a few tens of milliseconds. For a four-terminal

HVDC grid, the delay time is typically less than 200 ms. If the real power-controlled converters are reconnected before the voltage is stable, the system will encounter oscillations because the real power-controlled converters cannot maintain the rated voltage.

The restoration algorithm has been employed in the point-to-point HVDC test system with two HB converters. The restoration timeline is shown in Fig. 4.2. The changes in the DC voltage and real power of Converter 1 and Converter 2 during restoration are demonstrated in Figs. 4.3 (a)- 4.3 (b). The two ACCBs are closed at  $t = 40$  and  $t = 85$  ms, respectively. ACCB operation delay is considered. Converter 1 and Converter 2 are deblocked at  $t = 140$  ms and  $t = 172$  ms, respectively. The system restores its steady-state operation within one second.

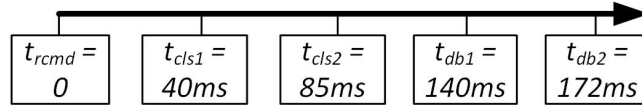


Figure 4.2: Restoration timeline of the HB point-to-point HVDC system.

- $t_{rcmd}$ : The instant at which the central-level controller sends the restoration command,
- $t_{iso}$ : DC disconnector opening instant,
- $t_{cls_i}$ : ACCB  $i$  closing instant, and
- $t_{db_i}$ : Deblocking instant of Converter  $i$ .

#### 4.2.2 Restoration of HVDC Systems with FB Converters

In an HVDC system consisting of only FB-MMCs, the opening and closing of ACCBs are not required during fault isolation and restoration, respectively. The delay time before deblocking the real power-controlled converters is also unnecessary as there is no uncontrollable current flow from the AC sides. The restoration timeline is shown in Fig. 4.4. The current and voltage waveforms during the restoration of the point-to-point HVDC test system with two FB converters are shown in Figs. 4.5 (a)- 4.5 (b). Converter 1 and Converter 2 are deblocked at  $t = 40$  ms and  $t = 41$  ms, respectively. The system restores its steady-state operation within 0.8 s.

### 4.3 Universal Restoration Algorithm for Hybrid MTDC Systems

When an HVDC grid consists of various types of converters, with and without fault blocking capability, the restoration algorithm should take into account the impact of each converter on the current and voltage waveforms. The main goal of the proposed universal

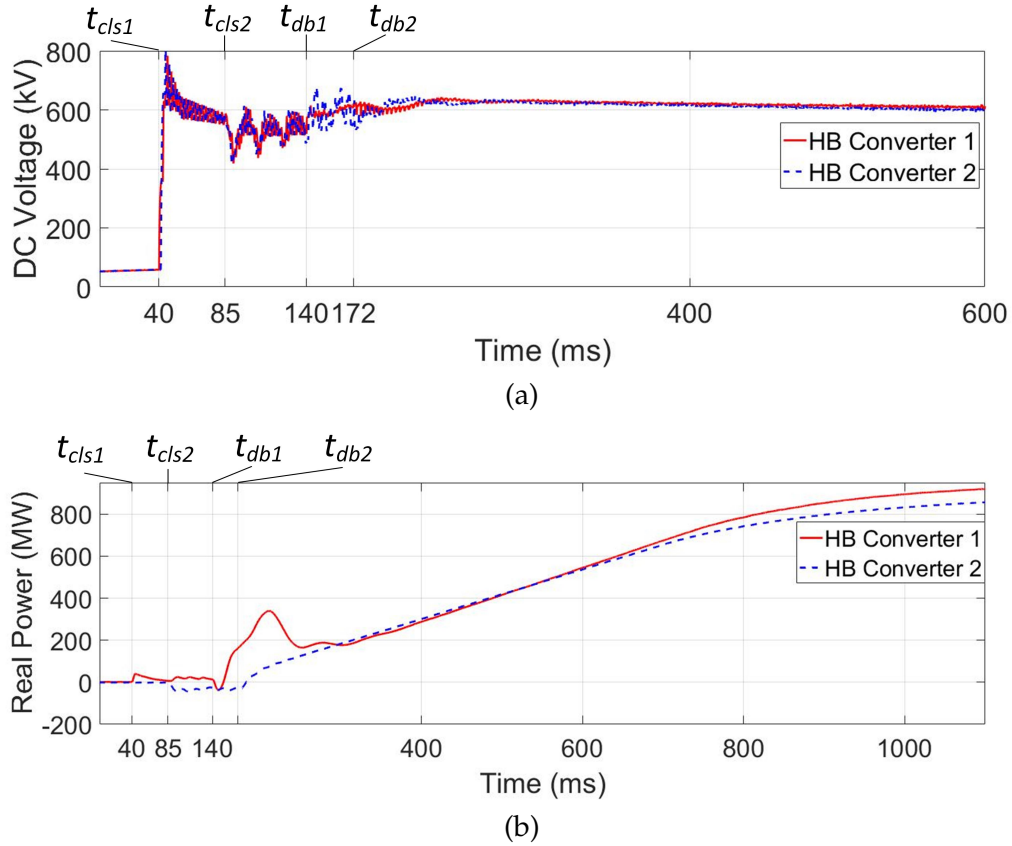


Figure 4.3: Restoration of HB point-to-point HVDC system: (a) DC voltage of Converter 1 and Converter 2 and (b) Real power of Converter 1 and Converter 2.

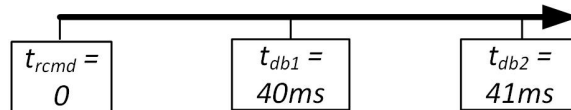


Figure 4.4: Restoration timeline of the FB point-to-point HVDC system.

restoration algorithm for hybrid HVDC grids is to improve the speed and reliability of the restoration process. The proposed universal restoration algorithm requires all the converter stations to operate individually during the restoration process. Based on the proposed algorithm, converter-level controllers restore the converters upon the satisfaction of the pre-defined restoration requirements. The local restoration of the converters, which is completed independently from the central-level controller, enables fast restoration of large-scale MTDC systems.

The proposed universal algorithm assumes that at the instant the central-level controller sends out the restoration commands to all converter-level controllers, all the converters are blocked and all ACCBs that are connected to HB-MMCs are open. In the

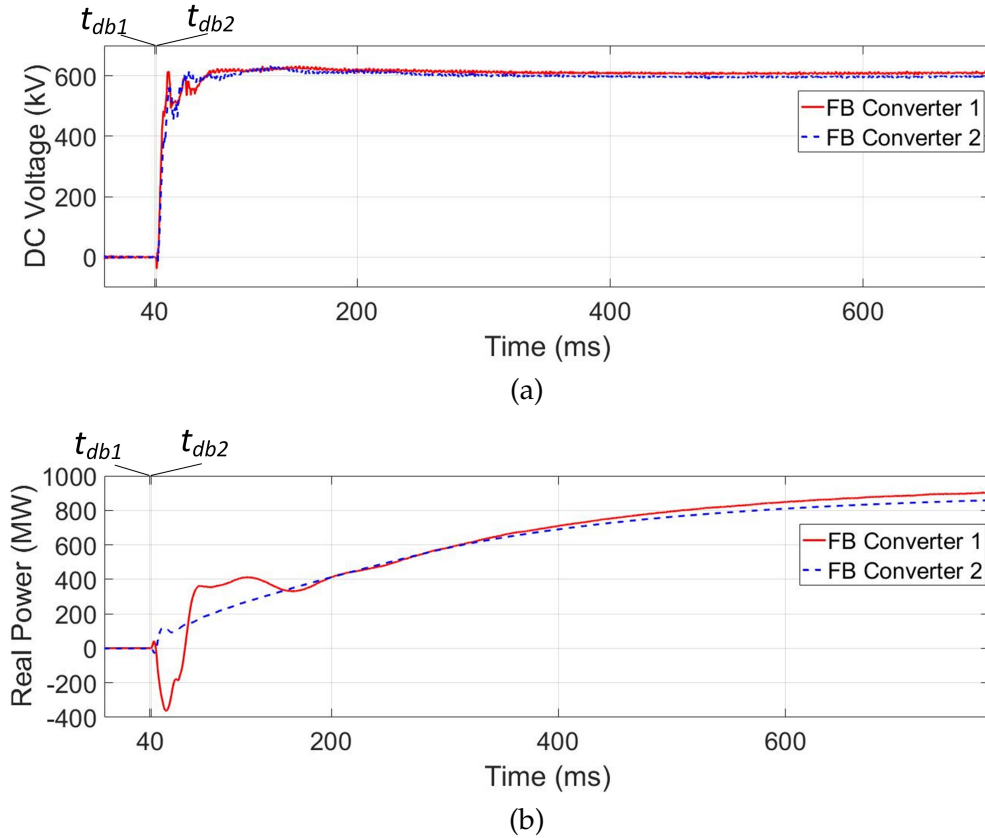


Figure 4.5: Restoration of FB point-to-point HVDC system: (a) DC voltage of Converter 1 and Converter 2 and (b) Real power of Converter 1 and Converter 2.

restoration algorithm proposed in [60], the system recovery can only start after the DC current in the DC grid has completely decayed to zero. However, in the restoration algorithm proposed in this thesis, restoration starts when the faulted transmission line is isolated by the MDs. At the opening instant of MDs, the DC current is not necessarily zero but must have reached a small value as the MDs can open when the current has a small value. Opening the MDs results in voltage oscillations in the DC grid, which consequently causes current oscillations with a small magnitude. The proposed universal algorithm comprises of the following steps:

- **Step 1: Fault clearance test:** This step is initiated upon receiving the restoration command from the central-level controller. In this step, the ACCB of one of the HB converters is closed to inject power to the DC grid. If the DC voltage reaches  $V_{TH1}$ , e.g., 80% of the AC peak voltage, for  $\Delta T_1$ , e.g., 10 ms, the restoration process will be continued.
- **Step 2: Closing of all ACCBs associated with HB-MMCs:** In this step, when the DC terminal voltage of any HB converter exceeds  $V_{TH1}$  for  $\Delta T_1$ , the converter-level controller of the HB-MMC closes the associated ACCB. After closing all the ACCBs

associated with HB converters, if the DC side voltage is relatively stable, the restoration process will continue.

- **Step 3: Restoration of all DC voltage-controlled converters:** In this step, after the DC terminal voltage remains above  $V_{TH2}$ , e.g., 95% of the AC peak voltage, for  $\Delta T_2$ , e.g., 100 ms, the DC voltage-controlled converters are deblocked and restored to their normal operation. The ideal case is to restore all DC voltage-controlled converters at the same time to expedite the restoration process. Although the DC voltage setting of the converters during the pre-fault operation may be different for power flow control purposes, during the restoration process, the DC voltage set-point of all the converters is considered to be the same as the reference DC voltage to minimize uncontrollable power flow among the converters.
- **Step 4: Restoration of all real power-controlled converters:** In this step, after the DC terminal voltage is stable and has remained above  $V_{TH3}$ , e.g., 95% of the rated DC voltage for  $\Delta T_3$ , e.g., 100 ms, the real power-controlled converters are deblocked and restored to their normal operation. At the end of this step, power transfer in all transmission lines is retrieved.
- **Step 5: Voltage setting adjustment:** In this step, the DC voltage setting of DC voltage-controlled converters is readjusted after a certain requirement is met. This requirement is associated with an input or output power threshold, i.e., power transmission reaches 50% of the rated power. At the end of this step, the MTDC system restores its steady-state operation.

The timeline of the proposed restoration algorithm is shown in Fig. 4.6. All the converters monitor their DC terminal voltages and when the preset requirements are met, the corresponding restorative actions are carried out. For all HB-MMCs, the requirement for closing their ACCBs is that the DC terminal voltage exceeds  $V_{TH1}$  for over  $\Delta T_1$ . For DC voltage-controlled converters, the requirement for deblocking the converter is that the DC voltage exceeds  $V_{TH2}$  for over  $\Delta T_2$ . For DC voltage-controlled HB-MMCs, the  $\Delta T_2$  can be selected to be longer than that of DC voltage-controlled FB converters by  $\Delta T_{HB}$ . This will enable the restoration of DC voltage-controlled FB-MMCs prior to DC voltage-controlled HB-MMCs. Restoring (deblocking) FB-MMCs before HB-MMCs reduces the current oscillations caused by uncontrollable AC contribution during the restoration process. For real power-controlled converters, the requirement for deblocking the converters is that the DC voltage exceeds  $V_{TH3}$  for over  $\Delta T_3$ , which ensures that the DC voltage-controlled converters are restored successfully before restoring real power-controlled converters. Similarly, deblocking the real power-controlled HB-MMCs after the real power-controlled FB-MMCs reduces the current oscillations during the restoration process.

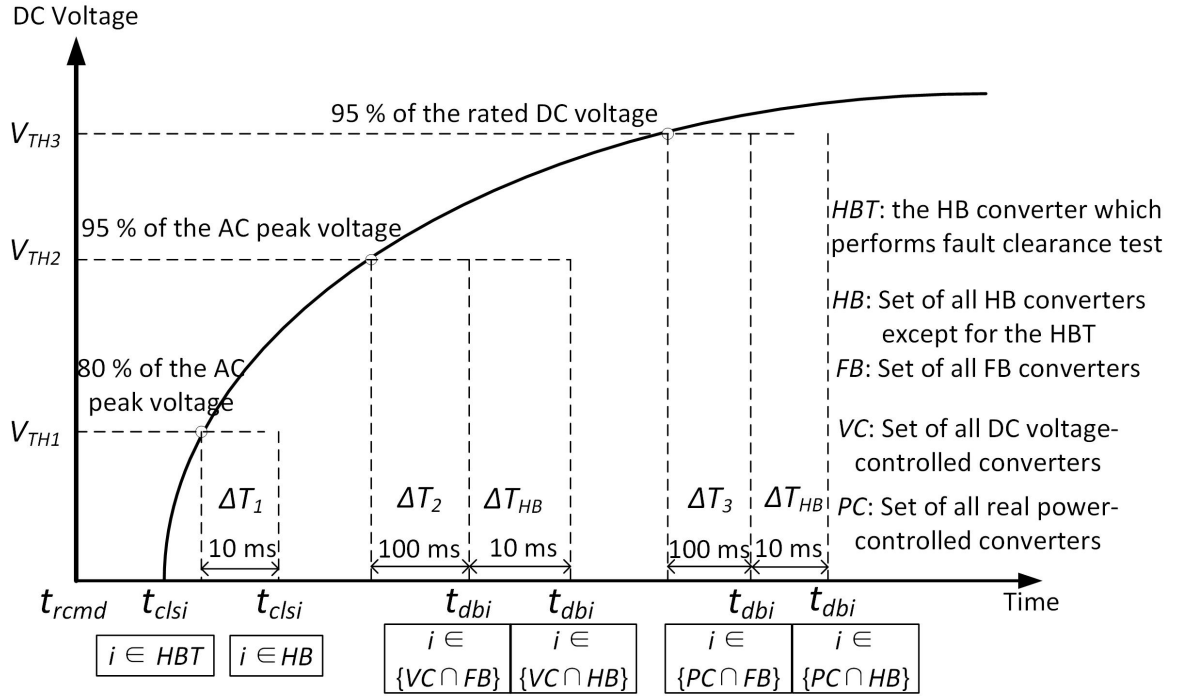


Figure 4.6: The proposed restoration algorithm.

In [33], the DC voltage threshold and the corresponding time duration required for deblocking of real power-controlled converters are selected to be 90% of the rated DC voltage and 20 ms, respectively. Such a voltage threshold and time duration are reasonable for a point-to-point HVDC system. If the DC grid contains more converter stations and longer transmission lines, this step of the restoration process will take longer. The proposed restoration algorithm of this thesis requires the ACCBs to close before deblocking the converters. However, the restoration algorithm proposed in [60] suggests that, for a weak AC grid, deblocking converters before closing the ACCBs can reduce the stress on the weak grid. However, operating an MMC without connection to the AC grid affects the voltage of SM capacitors. Furthermore, if the converter is deblocked while the ACCB remains open, the voltage oscillations will become significantly large.

The main advantages of the proposed universal restoration algorithm include:

- Fast restoration process due to the individual operation of all converters (independent from the central-level controller)
- Reliable restoration algorithm with properly set thresholds, and
- Applicability of the proposed restoration algorithm, paired with the proposed selective fault detection and isolation algorithm, to hybrid MTDC systems with any combination of converters with and without fault blocking capability.

## 4.4 Study Results for the Restoration of the Hybrid DC Systems

Following the proposed universal restoration algorithm, an MTDC system can be restored within one second after the fault is cleared. The performance of the proposed restoration algorithm is evaluated in this section.

### 4.4.1 Fault Clearance Test

In the hybrid MTDC system 1, Converter 2 and Converter 3 have HB SMs. In this study, Converter 3 is selected to perform the fault clearance test. When all the protective operations are completed, the central-level controller sends a signal to Converter 3 to close the ACCB. If the voltage of the DC grid is restored to a pre-defined value, as shown in Fig. 4.7, the fault clearance test is passed.

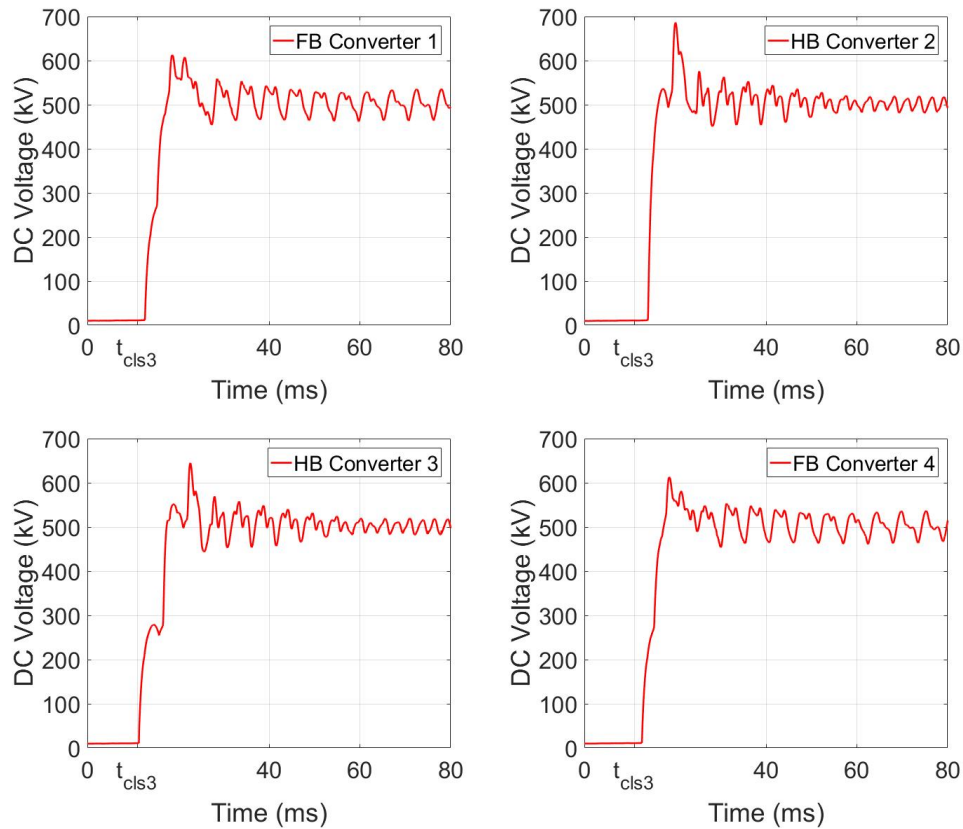


Figure 4.7: DC voltage of the four converters during a successful fault clearance test.

At  $t = 11$  ms, the ACCB of Converter 3 is closed and the DC voltage of all the converters rises up to 510 kV (the AC peak voltage) in about 10 ms. The DC side voltage of Converter 3 will eventually become a six-pulse waveform. This indicates that the system is clear of fault. In the test system, the DC voltage threshold of successful fault clearance test is 410 kV (80% of the AC peak voltage) for over 10 ms.

A failed fault clearance test is shown in Fig. 4.8. When the ACCB of Converter 3 closes at  $t = 11$  ms, the DC voltage rises up and then drops down. After 20 ms, the DC voltage does not reach the threshold value. The ACCB of Converter 3 is opened and the test failure information is sent to the central-level controller. The restoration unit should wait for a new fault clearance signal from the central-level controller to restart its operation. When the central-level controller receives a fault clearance test failure signal, fault detection and isolation will be conducted again.

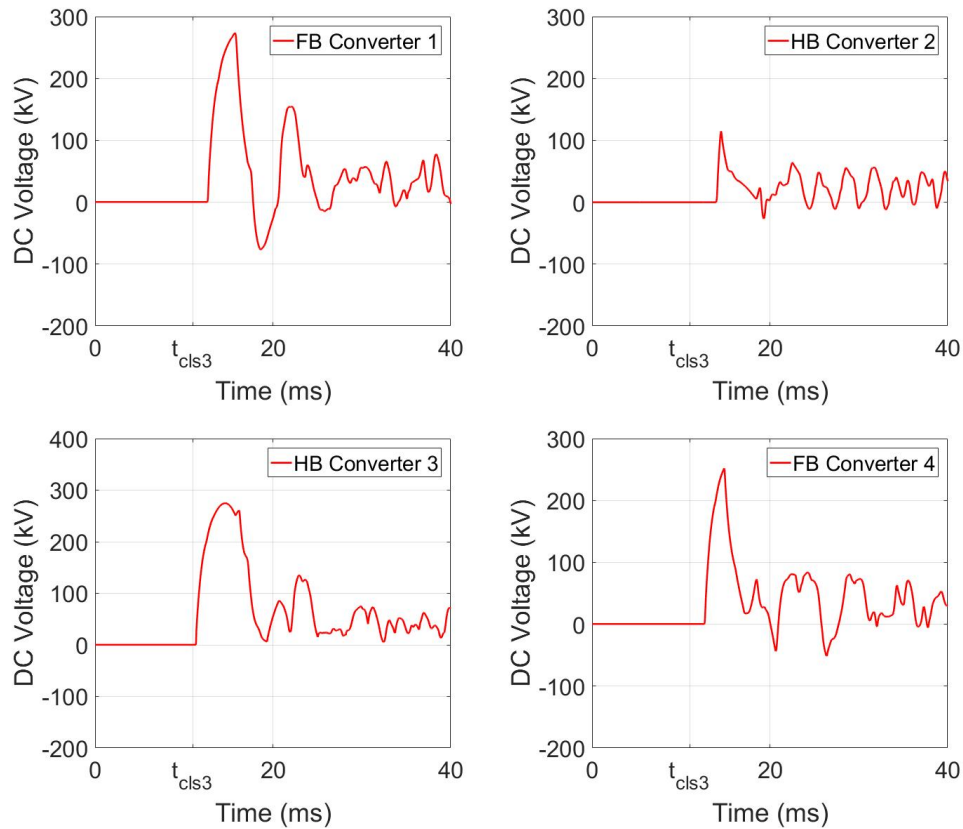


Figure 4.8: DC voltage of the four converters during a failed fault clearance test.

#### 4.4.2 Restoration of the Hybrid Point-to-Point HVDC System

In the hybrid point-to-point HVDC system, Converter 1 and Converter 2 have FB and HB SMs, respectively. After the fault clearance, the central-level controller sends the restoration command to the two converters at  $t = 0$  ms. At  $t = 50$  ms, the ACCB of Converter 2 is closed and the DC terminal voltage is restored to the AC peak voltage. When the voltage threshold (95% of the AC peak voltage) is reached at  $t = 156$  ms, Converter 1 is deblocked and the DC voltage is restored to the normal operating voltage. Converter 2 is deblocked at  $t = 288$  ms when the voltage threshold (95% of the DC operating voltage) is reached. The restoration timeline of the hybrid point-to-point HVDC system is shown in Fig. 4.9. The

DC voltage waveforms and power waveforms are shown in Fig. 4.10.

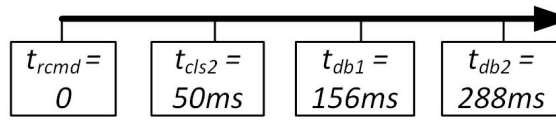
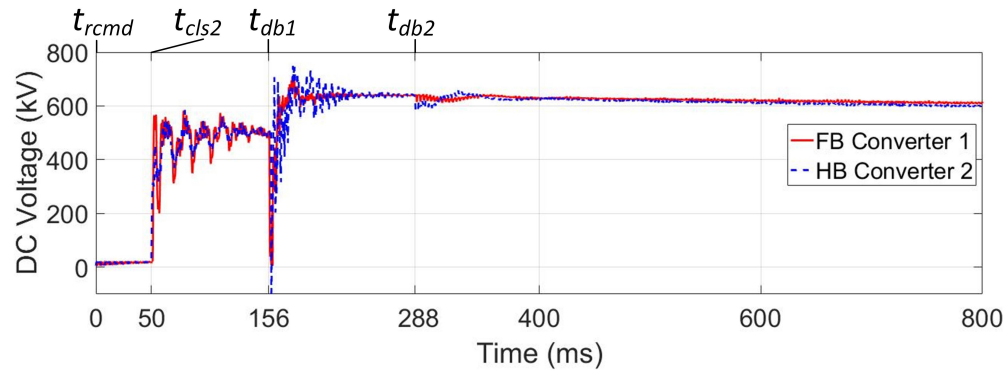
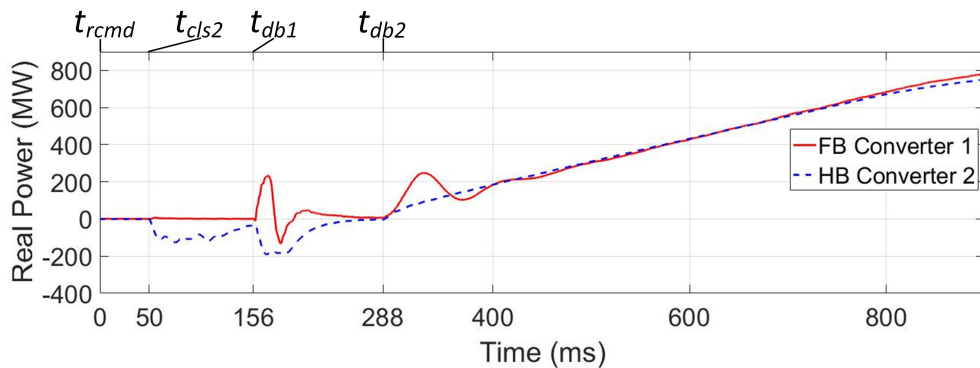


Figure 4.9: The restoration timeline of the hybrid point-to-point HVDC system.



(a)



(b)

Figure 4.10: Restoration of the hybrid point-to-point HVDC system: (a) DC voltage and (b) Real power.

In the simulation, all the restoration operations are triggered by comparators and integrator as shown in Fig. 4.11. When the DC voltage is higher than the voltage threshold, comparator 1 outputs a high level. The integrator's output value depends on the duration of the high level. When the level duration is longer than the time threshold, the corresponding operation is triggered by comparator 2. In the hybrid point-to-point system, the thresholds for the deblocking of Converter 1 are 485 kV and 20 ms for comparators 1 and 2, respectively. The thresholds for the deblocking of Converter 2 are 610 kV and 100 ms for comparators 1 and 2, respectively. The same trigger is used in all the restoration studies.

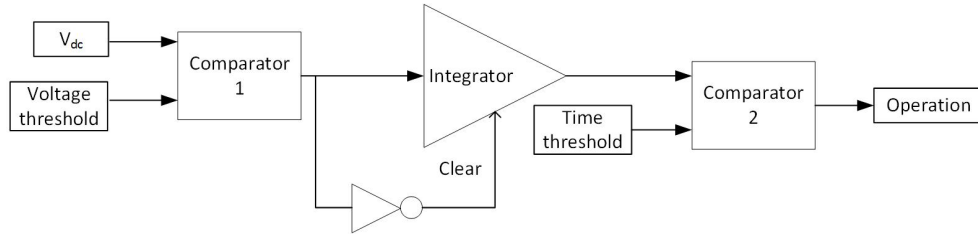


Figure 4.11: Trigger diagram in the simulation.

#### 4.4.3 Restoration of the Hybrid MTDC System

In this study, the four converters in the hybrid MTDC system 2 have FB, HB, HB, and HB SMs, respectively. T-line 2 is the faulted transmission line and is isolated. The restoration timeline is shown in Fig. 4.12. The results from the four-terminal MTDC test system restoration is shown in Fig. 4.13 and Fig. 4.14. The deblocking instant of the four converters as well as the closing instant of the three ACCBs are marked. In this study, the DC voltage-controlled Converter 4 is restored first, followed by Converter 1, Converter 3 and Converter 2. All the restoration operations are triggered by the pre-defined voltage and duration thresholds. The DC voltage of Converter 2 reaches the threshold later than Converter 3 as T-line 2 is disconnected.

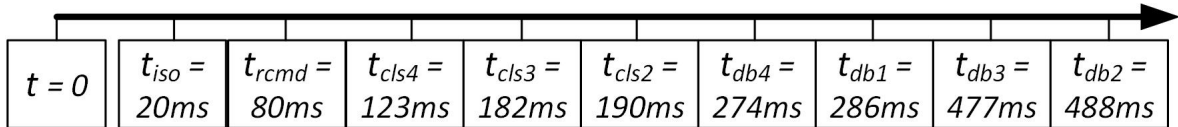


Figure 4.12: The restoration timeline of the hybrid four-terminal MTDC system.

In Figs. 4.13 and 4.14, the fault is isolated at  $t = 0$  ms. Isolating the faulted transmission line caused the DC voltage to rise up and oscillate at a certain level, depending on how much energy remains in the DC grid. The voltage oscillation is caused by the FB Converter 1, similar to stage 3 of the fault transient. In the restoration process, first, the ACCB connected to Converter 4 is closed at  $t = 123$  ms to perform the fault clearance test. As shown in Fig. 4.13, the voltage oscillation is eliminated by the fault clearance test. At  $t = 130$  ms, the DC system voltage reaches 510 kV. The ACCBs connected to Converter 2 and Converter 3 are closed at  $t = 190$  ms and  $t = 182$  ms, respectively as the pre-defined DC terminal voltage thresholds (485 kV for 100 ms) are met. Converter 1 and Converter 4 are restored at  $t = 274$  ms and  $t = 286$  ms, respectively. The DC voltage of the entire DC system reaches the pre-defined thresholds (605 kV for 100 ms) after 200 ms and Converter 2 and Converter 3 are restored at  $t = 488$  ms and  $t = 477$  ms, respectively. After all the restoration steps, the input and output power of all converters become stable and reach their pre-fault values after one second.

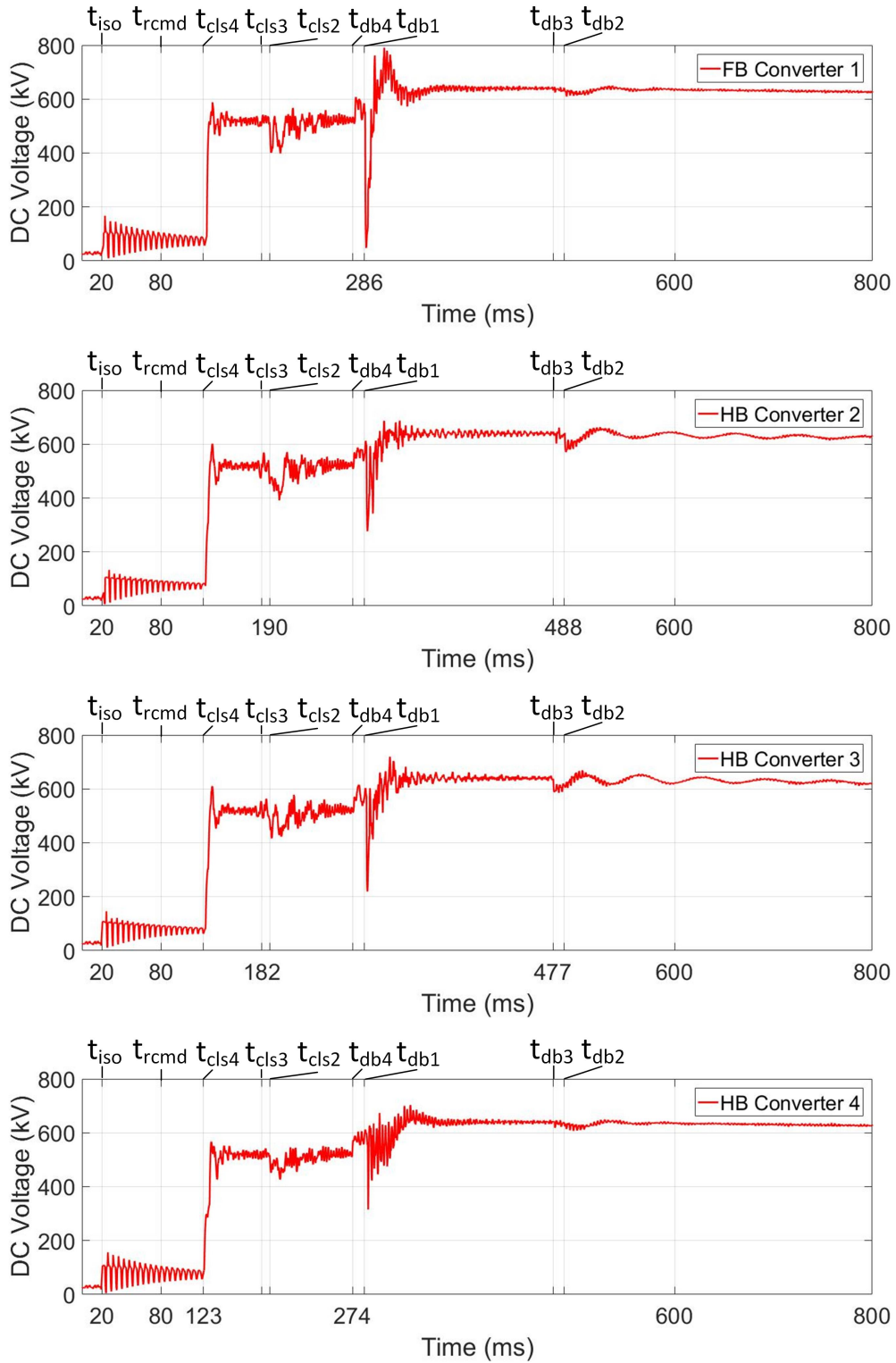


Figure 4.13: DC voltage of the four converters during restoration.

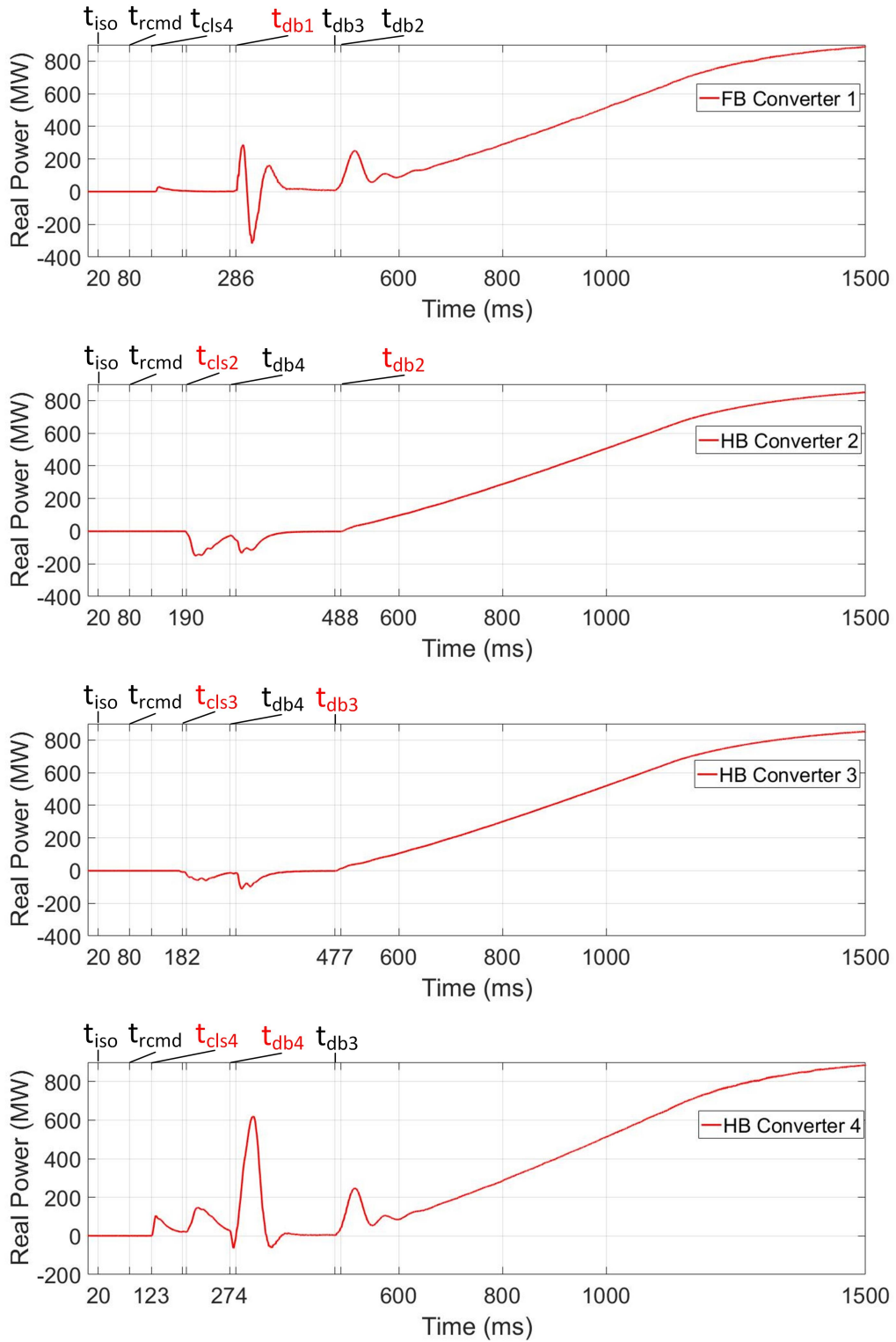


Figure 4.14: Real power of the four converters during restoration.

#### 4.4.4 Restoration Failure

There are two main reasons that may cause restoration failure in a hybrid MTDC system:

- **Fault isolation failure:** If the fault clearance test fails for a few times (e.g. 3 times), the fault clearance failure is reported to the central-level controller. The central-level controller will send an activation command to the fault detection and isolation unit.
- **Sustained current oscillation:** Failure to obtain a stable DC voltage when restoring real power-controlled converters. In such a case, all the real power-controlled converters will be blocked again. The restoration should restart from Step 3.

In the four-terminal MTDC test system 2, Converter 2 and Converter 3 have HB SMs and they are in real power control mode. During the restoration process, if Converter 2 and Converter 3 are restored based on the voltage threshold in the restoration algorithm proposed in [33], they will encounter voltage and current oscillations. The restoration timeline is shown in Fig. 4.15 and the voltage and current waveforms of the four converters are shown in Fig. 4.16.

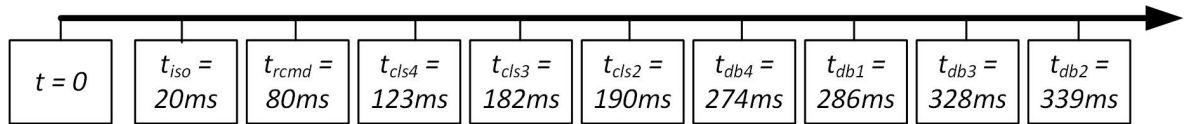
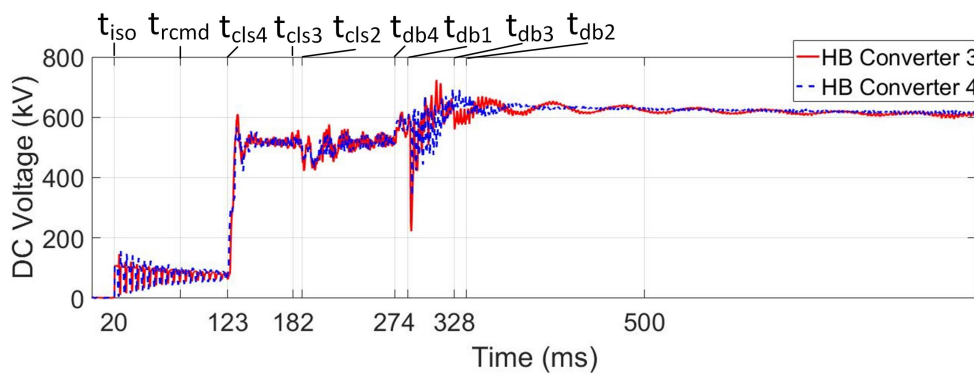
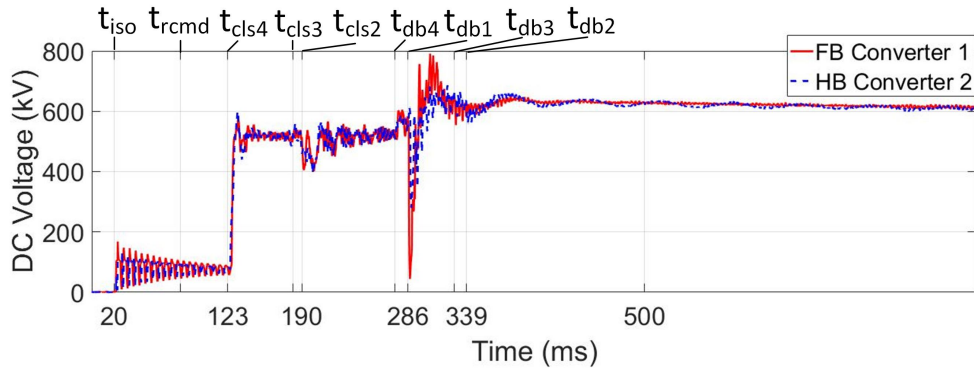


Figure 4.15: The restoration failure timeline of the hybrid four-terminal MTDC system.

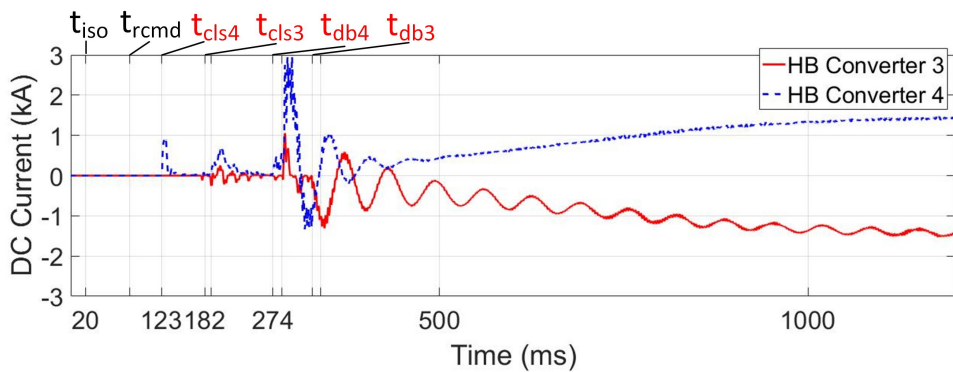
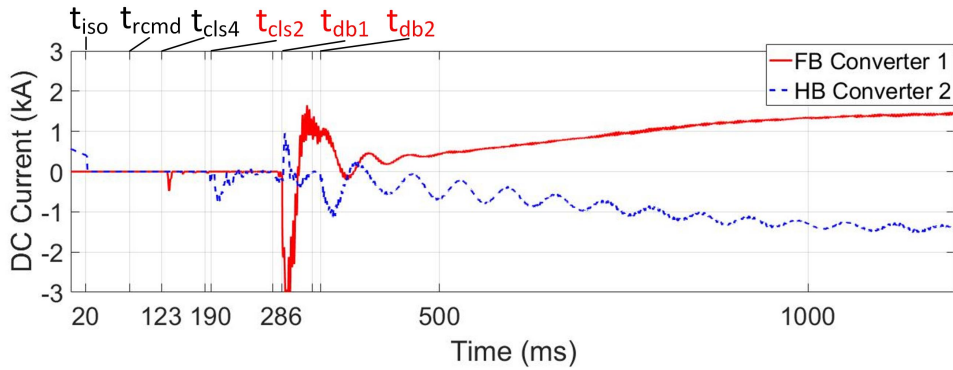
The operation of Converter 1 and Converter 4 are the same as the case study with a successful restoration. The voltage and real power waveforms of Converter 1 and Converter 4 are the same as the ones shown in Figs. 4.13 and 4.14. The differences between the two case studies is related to the operation of Converter 2 and Converter 3, which are respectively deblocked 149 ms and 150 ms earlier than the case with successful restoration. Untimely deblocking of the real power-controlled HB converters causes current oscillations in the converters.

## 4.5 Summary

This chapter summarized the restoration process of HVDC systems with only HB and FB converters with two case studies. A universal restoration algorithm that fits hybrid MTDC systems with various converters is proposed and verified with another two case studies. In all the restoration case studies, the hybrid point-to-point HVDC system and four-terminal MTDC system can restore the steady-state operations within 1 s after isolating the faulted lines. As a result, automatic and quick restoration after isolating the faulted lines can be achieved in MTDC systems.



(a)



(b)

Figure 4.16: Restoration failure of the hybrid MTDC system: (a) DC voltage of the four converters and (b) DC current of four converters.

# 5

## Conclusion and Future Work

### 5.1 Conclusion

This thesis addresses the major challenges in the protection of hybrid MTDC systems. In this thesis, the hybrid MTDC system modeling is discussed and a power flow control strategy is provided. The control of MTDC systems is divided into four levels. The central-level controller and converter-level controllers have individual responsibilities in the proposed protection algorithm. The differences between the fault transient response of FB and HB converters are studied in detail. Based on the fault transient study results, current derivatives are used to distinguish pole-to-pole and pole-to-ground faults. The central-level controller locates DC faults by analyzing the current directions and magnitudes of all the converters. The current difference between the two terminals of one transmission line is used to determine the existence of a pole-to-ground fault. Current direction analysis is also the preferred method to locate a pole-to-pole fault. After detecting and locating a DC fault, a permanent fault should be isolated by discharging the entire DC grid and opening the MDs. Finally, the healthy part of the MTDC system can be restored following the proposed restoration algorithm.

The proposed protection algorithm allows an MTDC system to ride-through DC faults automatically. The automatic protection algorithm enables MTDC systems to react faster in case of a DC fault. In all case studies, the healthy part of the MTDC system can be restored in less than two seconds after the fault instant.

## 5.2 Thesis Contribution

The main contributions of this thesis can be summarized as follows:

- Modeling of the hybrid MTDC systems and developing a power flow control strategy for MTDC systems.
- Pole-to-pole and pole-to-ground fault transient analysis of hybrid MTDC systems.
- The fault transient comparison between HB and FB VSCs.
- A selective fault detection and isolation algorithm is developed.
- A universal restoration algorithm design for hybrid MTDC systems.

## 5.3 Direction of Future Work

The following topics are proposed for future work:

- High voltage DCCBs are going to gain more attention in the future. As reliable and affordable high voltage DCCBs could change the protection scheme of MTDC systems, their impact on restoration of hybrid MTDC system must be studied.
- The development of fault locating algorithms which do not require communication.

# Bibliography

- [1] M. H. Rehmani, M. Reisslein, A. Rachedi, M. Erol-Kantarci, and M. Radenkovic, "Integrating renewable energy resources into the smart grid: Recent developments in information and communication technologies," *IEEE Transactions on Industrial Informatics*, vol. PP, no. 99, pp. 1–1, 2018.
- [2] A. L'Abbate, F. Careri, R. Calisti, and S. Rossi, "The impact of hvdc in the development of the pan-european system: Focus on italy-south east europe ties," in *2017 IEEE Manchester PowerTech*, pp. 1–6, June 2017.
- [3] E. E. U. European Commission, "Eu energy union and climate." [https://ec.europa.eu/commission/priorities/energy-union-and-climate\\_en](https://ec.europa.eu/commission/priorities/energy-union-and-climate_en). Accessed April 4, 2018.
- [4] T. Anderski, F. Careri, G. Migliavacca, N. Grisey, G. Sanchis, M. Gronau, K. Strunz, E. Peirano, A. Vafeas, and R. Pestana, "e-highway2050: Planning the european transmission grid for 2050," in *2016 IEEE International Energy Conference (ENERGYCON)*, pp. 1–6, April 2016.
- [5] E. N. of Transmission System Operators for Electricity, "Ten-year network development plan 2014." <https://www.entsoe.eu/publications/tyndp/tyndp-2014/>. Accessed April 4, 2018.
- [6] P. Kundur, N. J. Balu, and M. G. Lauby, *Power system stability and control*, vol. 7. McGraw-hill New York, 1994.
- [7] Canada, "Final report on the august 14, 2003 blackout in the united states and canada." <https://www3.epa.gov/region1/npdes/merrimackstation/pdfs/ar/AR-1165.pdf>. Accessed April 4, 2018.
- [8] M. M. Rahman, M. F. Rabbi, M. K. Islam, and F. M. M. Rahman, "Hvdc over hvac power transmission system: Fault current analysis and effect comparison," in *2014 International Conference on Electrical Engineering and Information Communication Technology*, pp. 1–6, April 2014.
- [9] Wikipedia, "High voltage direct current." [https://en.wikipedia.org/wiki/High-voltage\\_direct\\_current](https://en.wikipedia.org/wiki/High-voltage_direct_current). Accessed April 4, 2018.
- [10] W. A. Patterson, "The eel river hvdc scheme #x2014; a 320 mw asynchronous interconnection between the new brunswick electric power commission and hydro-qu #x00e9;bec employing thyristor valves," *Canadian Electrical Engineering Journal*, vol. 2, pp. 9–16, Jan 1977.

- [11] ABB, "Abb wins orders of over \$300 million for worlds first 1,100 kv uhvdc power link in china." <http://www.abb.com/cawp/seitp202/f0f2535bc7672244c1257ff50025264b.aspx>. Accessed April 11, 2018.
- [12] O. E. Oni, I. E. Davidson, and K. N. I. Mbangula, "A review of lcc-hvdc and vsc-hvdc technologies and applications," in *2016 IEEE 16th International Conference on Environment and Electrical Engineering (EEEIC)*, pp. 1–7, June 2016.
- [13] ABB, "First hvdc light." <http://new.abb.com/systems/hvdc/references/gotland-hvdc-light>. Accessed April 4, 2018.
- [14] H. Bilodeau, S. Babaei, B. Bisewski, J. Burroughs, C. Drover, J. Fenn, B. Fardanesh, B. Tozer, B. Shperling, and P. Zanchette, "Making old new again: Hvdc and facts in the northeastern united states and canada," *IEEE Power and Energy Magazine*, vol. 14, pp. 42–56, March 2016.
- [15] L. Zuiga-Garcia, A. Zaragoza-Hernandez, J. M. Nadal-Martnez, G. A. Anaya-Ruiz, E. L. Moreno-Goytia, L. E. Ugalde-Caballero, and V. Venegas-Rebollar, "Mmc technology and its participation in the integration of variable renewable energies and implementation of dc grids," in *2014 IEEE International Autumn Meeting on Power, Electronics and Computing (ROPEC)*, pp. 1–6, Nov 2014.
- [16] O. Gomis-Bellmunt, A. Egea-Alvarez, A. Junyent-Ferre, J. Liang, J. Ekanayake, and N. Jenkins, "Multiterminal hvdc-vsc for offshore wind power integration," in *2011 IEEE Power and Energy Society General Meeting*, pp. 1–6, July 2011.
- [17] N. R. Chaudhuri, R. Majumder, B. Chaudhuri, J. Pan, and R. Nuqui, "Modeling and stability analysis of mt dc grids for offshore wind farms: A case study on the north sea benchmark system," in *2011 IEEE Power and Energy Society General Meeting*, pp. 1–7, July 2011.
- [18] T. Augustin, I. Jahn, S. Norrga, and H. P. Nee, "Transient behaviour of vsc-hvdc links with dc breakers under faults," in *2017 19th European Conference on Power Electronics and Applications (EPE'17 ECCE Europe)*, pp. P.1–P.10, Sept 2017.
- [19] O. D. Adeuyi, N. Jenkins, and J. Wu, "Topologies of the north sea supergrid," in *Power Engineering Conference (UPEC), 2013 48th International Universities'*, pp. 1–6, Sept 2013.
- [20] T. M. Haileselassie and K. Uhlen, "Power system security in a meshed north sea hvdc grid," *Proceedings of the IEEE*, vol. 101, pp. 978–990, April 2013.
- [21] L. Huang, X. Yang, P. Xu, F. Zhang, X. Ma, T. Liu, X. Hao, and W. Liu, "The evolution and variation of sub-module topologies with dc-fault current clearing capability in mmc-hvdc," in *2017 IEEE 3rd International Future Energy Electronics Conference and ECCE Asia (IFEEC 2017 - ECCE Asia)*, pp. 1938–1943, June 2017.
- [22] Y. Tang, M. Chen, and L. Ran, "Design and control of a compact mmc submodule structure with reduced capacitor size using the stacked switched capacitor architecture," in *2016 IEEE Applied Power Electronics Conference and Exposition (APEC)*, pp. 1443–1449, March 2016.

- [23] E. Kontos, R. T. Pinto, and P. Bauer, "Providing dc fault ride-through capability to h-bridge mmc-based hvdc networks," in *2015 9th International Conference on Power Electronics and ECCE Asia (ICPE-ECCE Asia)*, pp. 1542–1551, June 2015.
- [24] W. Leterme, "Communication-less protection algorithms for meshed vsc hvdc cable grids," 2016.
- [25] H. Zhang, M. Wu, Y. Luo, G. Luo, J. He, and R. Li, "A novel transient-voltage based fault protection method for vsc-mtdc systems," in *2017 IEEE Conference on Energy Internet and Energy System Integration (EI2)*, pp. 1–5, Nov 2017.
- [26] M. M. Elgamasy, N. I. Elkalashy, T. A. Kawady, and A. M. I. Taalab, "Fault detection techniques for hvdc-vsc scheme using measurement at ac side," in *2017 Nineteenth International Middle East Power Systems Conference (MEPCON)*, pp. 876–880, Dec 2017.
- [27] R. C. Santos, S. Le Blond, D. V. Coury, and R. K. Aggarwal, "A novel and comprehensive single terminal ann based decision support for relaying of vsc based hvdc links," *Electric Power Systems Research*, vol. 141, pp. 333–343, 2016.
- [28] L. Tang and B. T. Ooi, "Locating and isolating dc faults in multi-terminal dc systems," *IEEE Transactions on Power Delivery*, vol. 22, pp. 1877–1884, July 2007.
- [29] Z. y. He and K. Liao, "Natural frequency-based protection scheme for voltage source converter-based high-voltage direct current transmission lines," *IET Generation, Transmission Distribution*, vol. 9, no. 13, pp. 1519–1525, 2015.
- [30] K. D. Kerf, K. Srivastava, M. Reza, D. Bekaert, S. Cole, D. V. Hertem, and R. Belmans, "Wavelet-based protection strategy for dc faults in multi-terminal vsc hvdc systems," *IET Generation, Transmission Distribution*, vol. 5, pp. 496–503, April 2011.
- [31] R. B. Junior, V. A. Lacerda, R. M. Monaro, J. C. M. Vieira, and D. V. Coury, "Selective non-unit protection technique for multiterminal vsc-hvdc grids," *IEEE Transactions on Power Delivery*, vol. PP, no. 99, pp. 1–1, 2017.
- [32] W. Leterme, P. Tielens, S. D. Boeck, and D. V. Hertem, "Overview of grounding and configuration options for meshed hvdc grids," *IEEE Transactions on Power Delivery*, vol. 29, pp. 2467–2475, Dec 2014.
- [33] E. Kontos, R. T. Pinto, and P. Bauer, "Fast dc fault recovery technique for h-bridge mmc-based hvdc networks," in *2015 IEEE Energy Conversion Congress and Exposition (ECCE)*, pp. 3351–3358, Sept 2015.
- [34] M. Hadjikypris and V. Terzija, "Transient fault studies in a multi-terminal vsc-hvdc grid utilizing protection means through dc circuit breakers," in *2013 IEEE Grenoble Conference*, pp. 1–6, June 2013.
- [35] N. Macleod, N. Cowton, and J. Egan, "System restoration using the "black" start capability of the 500mw eirgrid east- west vsc-hvdc interconnector," in *IET International Conference on Resilience of Transmission and Distribution Networks (RTDN) 2015*, pp. 1–5, Sept 2015.

- [36] B. Feng, X. Zhai, Y. Li, and Z. Wang, "Experimental study on black-start capability of vsc-hvdc for passive networks," in *2016 IEEE PES Asia-Pacific Power and Energy Engineering Conference (APPEEC)*, pp. 2560–2563, Oct 2016.
- [37] E. Kontos, R. T. Pinto, and P. Bauer, "Fast dc fault recovery technique for h-bridge mmc-based hvdc networks," in *2015 IEEE Energy Conversion Congress and Exposition (ECCE)*, pp. 3351–3358, Sept 2015.
- [38] CIGRE, "Cigre working group b4.57." <http://b4.cigre.org/content/download>. Accessed April 4, 2018.
- [39] Wikipedia, "Power system cad." [https://en.wikipedia.org/wiki/Power\\_systems\\_CAD](https://en.wikipedia.org/wiki/Power_systems_CAD). Accessed April 4, 2018.
- [40] U. N. Gnanarathna, A. M. Gole, and R. P. Jayasinghe, "Efficient modeling of modular multilevel hvdc converters (mmc) on electromagnetic transient simulation programs," *IEEE Transactions on Power Delivery*, vol. 26, pp. 316–324, Jan 2011.
- [41] M. Urrutia, A. Mora, A. Angulo, P. Lezana, R. Crdenas, and M. Diaz, "A novel capacitor voltage balancing strategy for modular multilevel converters," in *2017 IEEE Southern Power Electronics Conference (SPEC)*, pp. 1–6, Dec 2017.
- [42] M. Ricco, L. Mathe, and R. Teodorescu, "New mmc capacitor voltage balancing using sorting-less strategy in nearest level control," in *2016 IEEE Energy Conversion Congress and Exposition (ECCE)*, pp. 1–8, Sept 2016.
- [43] X. Shi, Z. Wang, L. M. Tolbert, and F. Wang, "A comparison of phase disposition and phase shift pwm strategies for modular multilevel converters," in *2013 IEEE Energy Conversion Congress and Exposition*, pp. 4089–4096, Sept 2013.
- [44] A. Ametani, "A general formulation of impedance and admittance of cables," *IEEE Transactions on Power Apparatus and Systems*, vol. PAS-99, pp. 902–910, May 1980.
- [45] S. Asha and N. Naoto, "A frequency-dependent model of a cabtyre cable for a transient analysis," *Journal of International Council on Electrical Engineering*, vol. 2, no. 4, pp. 449–455, 2012.
- [46] A. D. Shendge and N. N. Nagaoka, "A study on a cabtyre cable for a transient condition using electro magnetic transient program for switching surge application," in *2013 Asia-Pacific Symposium on Electromagnetic Compatibility (APEMC)*, pp. 1–6, May 2013.
- [47] N. Ray Chaudhuri, B. Chaudhuri, R. Majumder, and A. Yazdani, "Modeling, analysis, and simulation of ac–mtdc grids," *Multi-Terminal Direct-Current Grids: Modeling, Analysis, and Control*, pp. 77–151.
- [48] CIGRE, "A low loss mechanical hvdc breaker for hvdc grid applications." <https://library.e.abb.com/public/9242ee6dc653930bc1257d5d002f8484/A>. Accessed April 4, 2018.
- [49] D. Jovicic, M. Hajian, and L. Zhang, "Dc transmission grids with fault tolerant lcl vsc converters and mechanical dc circuit breakers," in *10th IET International Conference on AC and DC Power Transmission (ACDC 2012)*, pp. 1–6, Dec 2012.

- [50] ABB, "Zoning in high voltage dc (hvdc) grids using hybrid dc breaker." [https://library.e.abb.com/public/36de270ead191694c1257c01003445a0/Zoning%20in%20High%20Voltage%20DC%20\(HVDC\)%20Grids%20using%20Hybrid%20DC%20breaker.pdf](https://library.e.abb.com/public/36de270ead191694c1257c01003445a0/Zoning%20in%20High%20Voltage%20DC%20(HVDC)%20Grids%20using%20Hybrid%20DC%20breaker.pdf). Accessed April 4, 2018.
- [51] C. M. Franck, "Hvdc circuit breakers: A review identifying future research needs," *IEEE Transactions on Power Delivery*, vol. 26, pp. 998–1007, April 2011.
- [52] B. Mitra and B. Chowdhury, "Comparative analysis of hybrid dc breaker and assembly hvdc breaker," in *2017 North American Power Symposium (NAPS)*, pp. 1–6, Sept 2017.
- [53] J. Krishnan, H. Gueldner, K. Handt, and S. Nielebock, "A modular bi-directional hybrid circuit breaker for medium and high voltage dc networks," in *2016 18th European Conference on Power Electronics and Applications (EPE'16 ECCE Europe)*, pp. 1–9, Sept 2016.
- [54] B. Mitra and B. Chowdhury, "Comparative analysis of hybrid dc breaker and assembly hvdc breaker," in *2017 North American Power Symposium (NAPS)*, pp. 1–6, Sept 2017.
- [55] M. K. Bucher, M. M. Walter, M. Pfeiffer, and C. M. Franck, "Options for ground fault clearance in hvdc offshore networks," in *2012 IEEE Energy Conversion Congress and Exposition (ECCE)*, pp. 2880–2887, Sept 2012.
- [56] W. A. Elmore, *Protective relaying: theory and applications*, vol. 1. CRC press, 2003.
- [57] K. Sharifabadi, L. Harnefors, H.-P. Nee, S. Norrga, and R. Teodorescu, *Design, control, and application of modular multilevel converters for HVDC transmission systems*. John Wiley & Sons, 2016.
- [58] J. Liu, N. Tai, C. Fan, S. Chen, and P. Wu, "A fault detection method for dc lines in vsc-hvdc system based on current correlation," in *2016 IEEE Power and Energy Society General Meeting (PESGM)*, pp. 1–5, July 2016.
- [59] P. Pejovic, *Three-phase diode rectifiers with low harmonics: current injection methods*. Springer Science & Business Media, 2007.
- [60] P. Wang, X.-P. Zhang, P. F. Coventry, R. Zhang, and Z. Li, "Control and protection sequence for recovery and reconfiguration of an offshore integrated mmc multi-terminal hvdc system under dc faults," *International Journal of Electrical Power & Energy Systems*, vol. 86, pp. 81–92, 2017.
- [61] E. Veilleux and B. T. Ooi, "Multiterminal hvdc with thyristor power-flow controller," *IEEE Transactions on Power Delivery*, vol. 27, pp. 1205–1212, July 2012.
- [62] M. Ranjram and P. W. Lehn, "A multiport power-flow controller for dc transmission grids," *IEEE Transactions on Power Delivery*, vol. 31, pp. 389–396, Feb 2016.
- [63] M. Ndreko, M. Popov, and M. A. M. M. van der Meijden, "Short circuit current contribution from mtdc grids to the ac power system under ac system faulted conditions," in *11th IET International Conference on AC and DC Power Transmission*, pp. 1–8, Feb 2015.